A THESIS

FOR THE DEGREE OF DOCTOR OF PHILOSOPHY

A Meshless Method for Solving the Forward Problem of Electrical Impedance Tomography

Rong-Li Wang

Department of Nuclear & Energy Engineering

GRADUATE SCHOOL

JEJU NATIONAL UNIVERSITY

August, 2013

博士學位論文

EIT 에서 정문제를 위한 Meshless 방법

濟州大學校 大學院

에너지工學科

王榮麗

2013 年 08 月

EIT 에서 정문제를 위한 Meshless 방법

指導教授 金 信

王榮麗

이 論文을 工學 博士學位論文으로 提出함

2013 年 08 月

王榮麗의 工學 博士學位論文을 認准함

審査委員長 朴在雨 (인)

委 員 金慶淵 (인)

委 員 金南鎭 (인)

委 員 尹炳祚 (인)

委 員 金 信 (인)

濟州大學校 大學院

2013 年 08 月

A Meshless Method for Solving the Forward Problem of Electrical Impedance Tomography

Rong-Li Wang

(Supervised by Professor Sin Kim)

A thesis submitted in partial fulfillment of the requirement for the degree of Doctor of Philosophy

2013. 08

The thesis has been examined and approved.

.....

Thesis director, Jae-Woo Park, Professor, Department of Nuclear & Energy Engineering, Jeju National University

.....

Kyung-Youn Kim, Professor, Department of Electronic Engineering, Jeju National University

.....

Nam-Jin Kim, Associate Professor, Department of Nuclear & Energy Engineering, Jeju National University

.....

Byong-Jo Yun, Associate Professor, Department of Mechanical Engineering, Pusan National University

.....

Sin Kim, Professor, Department of Nuclear & Energy Engineering, Jeju National University

August, 2013

.....

Date

Department of Nuclear & Energy Engineering

GRADUATE SCHOOL

JEJU NATIONAL UNIVERSITY

REPUBLIC OF KOREA

Acknowledgements

This thesis is the result of work during my doctoral course whereby I have been supported by many people. It is my pleasure that I have now the opportunity to express my gratitude for all of them.

First of all, I would like to thank Professor Sin Kim for accepting me as a PhD student and supervising me throughout the entire course of the doctoral program. I feel extremely lucky to have Professor Sin Kim as my PhD supervisor and will always be appreciated of him for all his favors, kind support and supervision. His encouragement, guidance, support and kindness during my staying in Jeju have all been a source of motivation towards learning more and more. His thought-provoking seminars and discussions and a never-ending appetite for excellence I will admire and cherish for ever.

I am very grateful to Professor Kyung Youn Kim for his guidance, stimulating suggestions and continuous scrutiny of my research work. I would like to express my gratitude towards all the remaining members of my PhD advisory committee, Professor Jae-Woo Park, Professor Nam-Jin Kim, Professor Byong-Jo Yun, for agreeing to review my thesis and providing me the feedback to further improve my research work.

I am also grateful for the Department of Nuclear & Energy Engineering at Jeju University for providing me an excellent work environment during my study. I wish to offer my humble gratitude to all the professors of my department, for their extremely useful lectures, their guidance and invaluable comments during the course work.

I am fortunate enough to have chance to work with many people in my work group. I will never find words enough to express the gratitude that I owe to Dr. Anil Kumar Khambampati for his nonstop support and help, during the whole period of my stay in Jeju. I would always remember him for the deeply involved discussions we have had during this time. I am especially thankful to Dr. Bo-An Lee, for his kind help during my study and writing of the thesis, he has been so kind and helped me when ever I faced some difficulty in the work. I am much thankful to Dr. Bong-Seok

Kim for his help and advice during my research work. I always remember Murtuza Mehdi for he always motivated me to work and I never felt alone or stressed with work. Jeong-Seong Lee, Dr. Nauman Malik, Dong Liu, Yoon-Jeong Hong, Young-Jun Jang, Sung-Yong Lee, Ba-Ro Lee, and Min-Seok Ko have been good friends, they provided good support and were helpful in assisting me in numerous ways. I would like to thank all the other members in our work group, especially Dr. Yeon-Gun Lee, Yeon-Ha Park, Seung-Sin Kim and the secretaries of our lab, Ms Song, Ms Ko and Ms Mun, for their help and support in my thesis completion is highly gratified.

I would like to express my heartfelt thanks to Professor Paeng and Professor Cho, for their interesting and vivid interpretations in English Bible study. I will always remember the friends I met in the Bible class, the friendship and the enjoyable discussions with them had light up my years in Jeju.

I am glad to have friends in Jeju who always there for me when I need. Dr. Rui Zhang, Dr. Jin-Ji Wu, Dr. Ying Li, Dr. Fang-Meng Duan, Yao Chen, Lei Yang, Qi Kong, Xiao Liu, Cuong-Le, Ju-Ho Kim, Chang-Su Kim, Ji-Zhe Luo, Chul-Kyu Lim, Iskandar Makhmudov, Adnan Ali, Zahid Manzoor, Vivek Mathema, Kamran Ali, Qi Gu and Jin-Long Park are a few of those whose friendship help and support I would always admire. I thank them all for giving me so many memories to cherish during my stay in Jeju.

Finally, I would like to present my humble gratitude to my parents, my sister and other family members. All my professional and academic achievements, whatsoever, have been the result of their enormous efforts.

At the end I would like to thank all those whom I have not mentioned above but helped me in numerous ways to my success.

Abbreviations and notations

BC	Boundary condition
BDS	Boundary distributed source (method)
BEM	Boundary element method
BNM	Boundary node method
BPIM	Boundary point interpolation method
CEM	Complete electrode model
DLFS	Double layer fundamental solution
ECT	Electrical capacitance tomography
EFGM	Element-free Galerkin method
EIT	Electrical impedance tomography
FEM	Finite element method
GFEM	Generalized finite element method
IBDS	Improved boundary distributed source (method)
IIT	Inverse interpolation technique
LBIE	Local boundary integral equation
MLPG	Meshless local Petrov-Galerkin
MLS	Moving least-squares
MFS	Method of fundamental solution
MMFS	Modified method of fundamental solution
MMs	Meshless methods or mesh-free methods
MWLS	Meshless weighted least squares
PUFEM	Partition of unity finite element method
RBF	Radial basis functions
RKPM	Reproducing kernel particle method
RMM	Regularized meshless method
SBM	Singular boundary method
SLFS	Single layer fundamental solution
SPH	Smooth particle hydrodynamics
A	Magnetic vector potential, Stiffness matrix

a	Distance of the field point and source point in BDS
$A^{(i)}(s_j, x_i)$	Radial basis functions in MMFS
$\mathbf{A}$	Coefficient matrix
B	Magnetic induction, Component of stiffness matrix
C	Component of stiffness matrix
c	Constant used in RMM, SBM
D	Electric displacement, Component of stiffness matrix, Inclusion
∂D	Boundary of inclusion
E	Electric field, Electrode
e_l	l th electrode
$\lvert e_j \rvert$	Area of the j th electrode
g_l	l th gap
G	Fundamental solution of Laplace equation for Dirichlet boundary condition, Gap
$\tilde{G}$	Integration of the G on a circular disk
H	Magnetic field
I_{M_E}	Identity matrix
I_l	Current applied to the l th electrode
i, j	Indices
J	Current density
J^s	Current source
K	Matrix in BEM
L	Number of electrodes
l_j	Length of the j th segment on the boundary
M	Measurement matrix, Total number of segments
m_E	Number of segments on each electrode
m_G	Number of segments on each gap
M_D	Number of the segments of the inclusion boundaries
M_E	Total number of segments on electrodes

M_G	Total number of segments on gaps
$\widetilde{M}$	Extended measurement matrix
N	Number of nodes in the finite element mesh
$\widetilde{N}$	Extended mapping matrix
n_j	Normal vector at source point s_j
$\overline{n}_i$	Normal vector at field point x_i
P	Number of current patterns
p , p_i	Field point used in FEM, BEM, IBDS and hybrid MM
p_s , p_j	Source point used in BEM, IBDS and hybrid MM
Q	Expression of Neumann Boundary condition based on fundamental solution of Laplace equation
$\tilde{Q}$	Integration of the Q on a circular disk
$q_b(p)$	Normal derivative of potential on the background
$q_a(p)$	Normal derivative of potential on the inclusion
q_{ii}	Diagonal elements of the SBM interpolation matrix for Neumann boundary condition
$\overline{q}$	Given continuous functions for Neumann boundary
R_j , R_s	Radius of the distributed source in BDS, IBDS and hybrid MM
R	Radius of the circular domain
r	Distance from field point and source point
s_E	Sizes of the electrode segments
s_G	Sizes of the gap segments
s , s_j	Source point used in MFS, MMFS, RMM, SBM and BDS
t	Index of the boundary in RMM
u, $u(p)$,$u(\mathrm{x})$	Potential distribution inside an object
u^h	Approximation of potential distribution
u^*	Fundamental solution of two-dimensional Laplace equation used in RMM
u_{ii}	Diagonal elements of the SBM interpolation matrix for

	Dirichlet boundary condition
u^{*c}	Fundamental solution of the exterior problems
$u_a(p)$	Potential distribution on the inclusion of the object
$u_b(p)$	Potential distribution on the background of the object
$\bar{u}$	Given continuous functions for Dirichlet boundary
U^h	Approximation of boundary voltages
$\hat{\mathbf{U}}$	Voltages from the measurement electrodes
U_l, V_l	Voltage on l th electrode
w_j	Coefficients which need to determined in MFS
x, x_i	Field point used in MFS, MMFS, RMM, SBM and BDS
x_0	An arbitrary point inside the domain
x, y	Two components of the points in 2D plane
z_l	Contact impedance of l th electrode
α_i, β_i	Parameters used in FEM and MMs formulation
α_j'	Source densities for the points in SBM
δ	Dirac delta function
ε	Permittivity
θ	Model parameters
κ	Ratio between conductivity of Inclusion and background
μ	Permeability
μ_j^b	Source densities for the points on the background
μ_j^a	Source densities for the points on the inclusion
$\bar{\mu}_j$	Source densities for the arbitrary known particular solution in IBDS
$\boldsymbol{\mu}$	Density vector
ν	Outward unit normal
σ	Conductivity
σ_a	Conductivity of inclusions
σ_b	Background conductivity

ϕ_i	Two-dimensional first-order basis function
Ω	Object to be considered in the EIT problem
$\partial\Omega$	Boundary of the object
$\partial\Omega_G$	Boundary of the object on gap region
$\partial\Omega_E$	Boundary of the object on electrode region
$\partial\Omega_{E_i}$	i th segment of the electrode region
$\partial\Omega_{G_i}$	i th segment of the gap region
$\partial\Omega_t^{\bar{u}}$	Dirichlet boundary of the t th boundary in RMM
$\partial\Omega_t^{\bar{q}}$	Neumann boundary of the t th boundary in RMM

Contents

List of Figures

요약

Meshless methods 또는 Mesh-free methods (MMs)는 Mesh 에 기반한 방법들의 단점을 피하기 위해 계발된 수치적 방법들의 일종이다. MMs 에서, 근사치는 Nodes 에서만 만들어지므로, MMs 는 내부 경계를 포함하는 문제들에 특히 적합하다. MMs 중에서, Method of fundamental solutions (MFS)는 많은 공학 영역과 과학 영역에서 주목 받고 있다. MFS 에서는 지배 미분 방정식의 기본해를 선형결합 시킴으로써 문제를 해결한다. 그러나, 기존 MFS 는 물리 영역 외부에 소스점 (Source point)이 위치할 가상적인 경계가 필요하기 때문에, 가상 경계를 결정하는 것은 문제를 푸는데 있어서 중요하다. 기존 MFS 의 한계점을 극복하기 위해서, Modified method of fundamental solution (MMFS), Singular boundary method (SBM), Boundary distributed source (BDS) 방법 등과 같은 여러 수치 방법들이 제안되었다. MMFS, SBM, BDS 방법들은 물리 경계에 소스점들을 분포시킴으로써 기존 MFS 의 가상 경계 문제를 해소할 수 있다. SBM 방법의 요점은 역보간법 (Inverse interpolation method) 뿐만 아니라 Subtracting and adding-back technique 에 기반하는 기본해의 특이점을 구분시키는 Origin intensity factor 를 평가하는 것이다. BDS 방법의 핵심 개념은 이차원(2D)의 원 또는 삼차원(3D)의 구 위에 분포소스 (distributed source)를 고려함으로써 소스점들에서 기본해의 특이점들 (singularities)을 피하는 것이다. 향상된 BDS 방법, 즉 IBDS 방법은 전압의 보통 기울기를 적분해서 Neumann 경계 조건들에서의 대각 요소들을 결정하는 단순한 방법이다.

전기 임피던스 단층촬영 (Electrical Impedance Tomography; EIT) 은 영역 경계에 부착된 전극들에 전류를 인가하고, 이것으로부터 유도되는 전압 측정값을 이용하여 다른 전기 전도도를 갖는 매질의 형태와 위치를 복원하는 영상화 기술이다. EIT 정문제 (Forward problem)는 적분 형태의 제약들이 있는 혼합 경계 조건들에 지배되는 Laplace 방정식의 일종이다. 이것은 영역

재구성 또는 형태 재구성을 통해 전도도 분포를 결정하는 산업 단층 장비와 의료 단층 장비에 적용할 수 있다.

이 연구는 EIT 정문제를 수치적으로 풀기 위해서 SBM 방법과 IBDS 방법을 조합한 새로운 MM 을 제시하고 있다. SBM 방법에 쓰이는 역보간법은 Dirichlet 경계 조건들의 대각 요소들을 결정하기 위해 사용된다. IBDS 방법 뿐만 아니라 SBM 방법과 IBDS 방법을 조합시킨 새로운 MM 도 채택함으로써, Complete electrode model (CEM)에 대한 EIT 정문제의 수학적 공식을 얻을 수 있었다. 여러 수치적 예제들은 BEM 과 FEM 의 값과 비교함으로써 새로운 공식의 실용성과 정확성을 입증하기 위해 쓰였다.

결과들을 통해서 SBM 방법과 IBDS 방법을 조합한 MM 의 정확성이 IBDS 방법보다 낫다는 것을 알 수 있다. 게다가, IBDS 방법과 조합한 MM 둘 다 어떠한 복잡 기하구조 문제에 대해서도 아주 효과적이라는 것을 알 수 있었다. IBDS 방법과 비교해보면, 조합한 MM 은 높은 정확성을 보였고 소스점들의 반지름에 덜 의존적이었다. 바꿔 말해, 조합한 MM 이 더욱 효과적이고 더욱 안정적이라고 할 수 있다. 그러므로, 이 방법이 EIT 의 다양한 응용 사례에 적용될 수 있을 것으로 기대된다.

1. Introduction

1.1 Electrical impedance tomography

Electrical impedance tomography (EIT) is a non-intrusive method that reconstructs the electric conductivity distribution inside the domain of interest (Vauhkonen 1997). In EIT, a set of electrical currents is injected through an array of electrodes attached on the boundary of the object and the voltages are measured from the surface of the electrodes. Based on the current-voltage relationship, internal distribution inside the object is reconstructed. Schematic diagram which explains the principle of EIT is shown in figure 1.1.

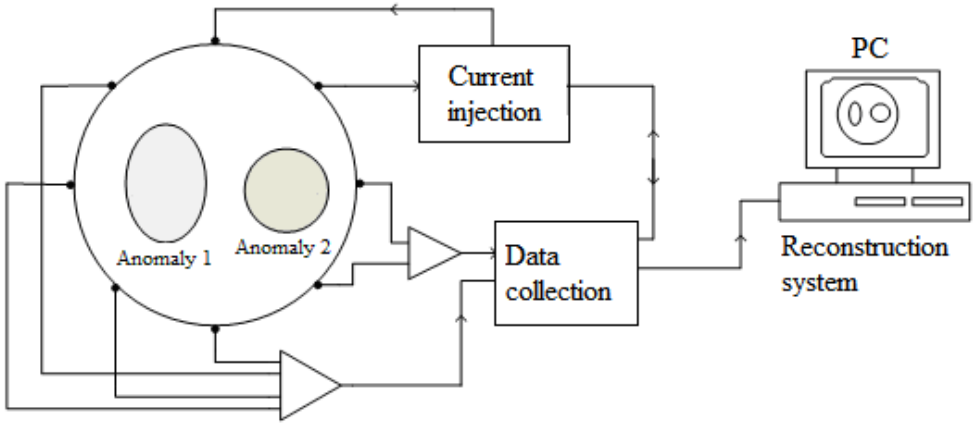

Figure 1.1. Schematic diagram which explains the principle of EIT.

EIT has lower spatial resolution, since EIT comes under soft field imaging techniques as the electrical quantities are dispersed inside the object and are effected by the inside objects. The main advantage with EIT is that it has low cost, convenient and safe. Apart from that, EIT has high-speed data collection system thus has high temporal characteristics. EIT has been applied in several fields of science and

engineering. In medical imaging, EIT can be used to detect tumors from breast tissue (Osterman 2000, Kim 2007), and monitor physiological phenomena, such as cardiac, pulmonary and respiratory functions (Harris 1991, Brown 1994, Deibele 2008, Somersalo 1992). EIT has been applied to clinical applications, like lung imaging (Brown 2001, Mueller 2001), head imaging (Holder 1992) and breast imaging (Cherepenin 2001, Cherepenin 2002, Kerner 2002(a), Kerner 2002(b), Osterman 2000) for instance. The applications of EIT in the process industry include monitoring of flow processes, monitoring of the mixing phenomenon and multiphase flows and non destructive measurements (Mann 1997, Kim 2005, Khambampati 2009, Rashid 2010a, Dickin and Wang 1996, Pinheiro 1997, Jones 1993, Friedman 1989). In the application of EIT in geophysics, resistivity reconstruction is widely used in exploring mineral resources, ground water, detection of fractures, contaminant plumes, waste dumps, geological mapping, geotechnical and environmental applications (Maillol 1999, Barker 1998, Daily 1992, Spies 1995).

In EIT, the physical relationship between the injected currents and the measured boundary voltages is governed by a partial differential equation derived from Maxwell equations. There are many physical models that can be considered, such as continuum model (Cheng 1989, Somersalo 1992), average-gap model (Somersalo 1992), shunt model (Somersalo 1992) and complete electrode model (CEM) (Somersalo 1992, Vauhkonen 1997). Compared to other physical models, CEM is modeled by considering the discreteness, shunting and contact impedance between electrode and electrolyte. Therefore, it is close to real situation and gives a better approximation of boundary voltages on electrodes. EIT includes forward and inverse problem. The forward problem is to calculate the potential distribution for a known distribution of conductivity subjected to appropriate boundary conditions. The inverse problem is to estimate the internal conductivity distribution inside the domain based on the current-voltage relationship. For homogenous case, analytical solution for EIT forward problem has been presented (Kim 2007). For complex geometry, it is difficult to obtain analytical solution therefore numerical methods are often used. Currently, the EIT forward problem solvers are mainly based on finite element methods (FEM) (Vauhkonen 1997, Polydorides 2002, Andrew 2003). Another

numerical method which has been used for solving forward problem of EIT is the boundary element method (BEM) (also known as the boundary integral method) (Duraiswami 1997, de Munck 2000, Khampampati 2011, Khampampati 2012).

1.2 Meshless methods

The Finite Element Method (FEM) and Boundary Element Method (BEM) may be the most well-known numerical methods of these thoroughly developed mesh-based methods. In contrast, to avoid the disadvantages of numerical methods based on mesh, a comparably new class of numerical methods has been developed which approximates the solution of partial differential equations only based on a set of nodes without the need for an additional mesh, called Meshfree Methods or Meshless Methods (MMs).

Since only a cloud of nodes is required, the MMs are particularly suitable for complex geometry problems. Zhang *et al.* (2010) had reported in their work about the numerical simulation of forward problem for electrical capacitance tomography (ECT) using element-free Garlerkin method (EFGM) in which a shape function is constructed by moving least-squares (MLS) approximation, a variational equation weak form of the studied problem is used to deduce the discrete equation, and Lagrange multipliers are used to satisfy the essential boundary conditions.

One of the first MM is the smooth particle hydrodynamics (SPH) method proposed by Lucy (1977) and Gingold and Monaghan (1977), which was used to solve problems in astrophysics and in fluid dynamics (Monaghan 1982, Monaghan 1988, Bonet 2000). Since the original SPH version suffered from spurious instabilities and inconsistencies (Swegle 1995, Xiao 2005, Belytschko 2000), many improvements were incorporated into SPH (Belytschko 1996, Bonet 2000, Johnson 1996, Johnson 2000, Randles 1997, Vila 1999, Rabczuk 2004). Since SPH and their corrected versions were based on a strong form, other methods based on a weak form were developed in the 1990s (Belytschko 1996).

The MMs can be categorized in a number of ways. One possible categorization is by the type of weak forms. The EFGM (Belytschko 1994) developed in 1994 was one of the first MM based on a global weak form. The reproducing kernel particle method (RKPM) (Liu 1995) was developed in 1995. RKPM has its origin in wavelets, but the final equations of RKPM were very similar to the equations of the EFGM. In contrast to RKPM and the EFGM, other methods were developed by using an extrinsic basis and the partition of unity concept. This extrinsic basis was initially used to increase the approximation order similar to a prefinement as, *e.g.* in the *hp*-cloud method (Bonet 2000). Melenk and Babuˇska (1996) pointed out the similarities between MMs and FEM and developed the partition of unity finite element method (PUFEM). The method is very similar to the *hp*-cloud method. Generally, PUFEM shape functions are based on Lagrange polynomials, while the general form of the *hp*-cloud method also includes the MLS-approximation. Strouboulis *et al.* (Strouboulis 2000) pointed out in their generalized finite element method (GFEM) that different partition of unities can be used for the usual approximation and the enrichment.

Most of the above MMs which based on global weak forms that usually require background cells for integration. Strictly speaking, these MMs require background cells for integration are not truly MMs (Wang 2009). In order to avoid any mesh with both interpolation and integration, local weak forms or collocation methods was involved such as those MMs based on a local boundary integral equation (LBIE) (Atluri 1998, Zhu 1998) or collocation meshless methods (Kansa 1990, Wang 2009). The most popular method is the meshless local Petrov–Galerkin (MLPG) method (Atluri 1998, Wang 2002, Atluri 2005). The main difference of the MLPG method to methods such as EFG or RKPM is that local weak forms are generated on overlapping subdomains other than using global weak forms. The integration of the weak form is then carried out in these local subdomains. Atluri (2002) introduced the notion “truly” meshless since no construction of a background mesh is needed for integration purposes.

Another way of categorization is by the type of integration domain:

(i) boundary type methods such as the boundary node method (BNM) (Mukherjee 1997, Chati 1999), method of fundamental solution (MFS) (Young 2005, Young 2006, Chen 2006, Chen 2012) and boundary point interpolation method (BPIM) (Gu 2002) ;
(ii) domain type methods which include all other MMs, like meshless weighted Least squares (MWLS) method (Liu 2005, Bodin 2006).

The most attractive merits of the MMs are:
(i) they provide an alternative numerical tool, free from extensive and costly mesh generation;
(ii) they can be used for dealing with complex geometries, and are easily extendible to multi-dimensional problems.

Beside these merits, MMs are not without demerits. Some of the MMs shape functions are rational functions which requires high-order integration scheme to be correctly computed. The treatment of essential boundary conditions is not as straightforward as in mesh-based methods. To avoid some difficulties inherent in MMs, MMs were coupled successfully to mesh-based methods (Belytschko 1995, Fernandez 2001, Fernandez 2003, Fernandez 2004, Huerta 2000, Huerta 2004, Nguyen 2008). Meanwhile, hybrid methods are available that take the advantages of both meshfree methods and finite elements (Hao 2006, Liu 2004, Idelsohn 2004, Rabczuk 2004, Chinnaboon 2007) , *e.g*. the shape functions fulfill the Kronecker delta property while simultaneously exploiting the smoothness and higher-order continuity of meshfree shape functions. Common issues in MMs are approximation, integration of the weak form, imposing essential boundary conditions, how to compute shape functions and how to incorporate strong and weak discontinuities. In addition, the weighted residual methods such as collocation and Galerkin procedures are also stated with examples. Other surveys on MMs can be found in (Belytschko 1996) and in (Li 2002). Special issues of journals on various aspects of MMs may be found in (Liu 1996, Chen 2000, Chen 2004). A few books on MMs are also available, for *e.g.* (Alturi 2002, Griebel 2002, Liu 2002, Fries 2004) .

1.3 Aims and contents of the thesis

The purpose of this thesis is to develop novel meshless method (MM) for solving the EIT forward problems. Among the mesh-free methods, the Method of Fundamental Solutions (MFS) has gained an increasing attention in many engineering and science fields (Mathon 1977, Rek 1999, Young 2005, Young 2006, Sarler 2009, Chen 2006, Chen 2012). The MFS approximates the solution of the problem as a linear combination of fundamental solutions of the governing differential operator. However, the conventional MFS requires a fictitious boundary outside the problem domain to place the source points due to singularity of the fundamental solution (Mathon 1977, Young 2005, Sarler 2009). The determination of fictitious boundary is not trivial (Sarler 2009). To overcome this main drawback of the MFS, several methods such as the Modified Method of Fundamental Solutions (MMFS) (Young 2005, Young 2006, Chen 2006, Sarler 2009), the Singular Boundary Method (SBM) (Chen 2010, Gu 2012, Chen 2012), and the Boundary Distributed Source (BDS) method (Liu 2010, Perne 2012, Kim 2013) have been proposed. Among these, we consider the BDS method for the EIT forward problem. The main idea of the BDS is to avoid the singularities of the fundamental solution at source points by considering a distributed source over circles in 2D or spheres in 3D.

In this study, the BDS methods extended to solve the forward problem of EIT. The basic BDS formulation for solving EIT forward problems is developed. 2-D examples including homogenous case and inhomogeneous case are presented with the numerical results compared with BEM and FEM.

This thesis contains five chapters. Chapter 1 gives a brief introduction about EIT, its applications and methodology. It also presents the introduction of MMs, including characteristics of some widely used MMs.

Chapter 2 deals with the mathematical models used in solving EIT forward problem. Complete electrode model which is used as the physical model in the thesis is explained. Finite element formulation based on CEM is explained briefly.

Boundary element method for solving the forward problem of EIT is introduced with CEM model, the numerical results is used for the comparison.

In chapter 3, different kinds of MMs are studied. Such as method of fundamental solution (MFS), modified method of fundamental solution (MMFS), singular boundary method (SBM) and boundary distributed source (BDS) method.

Chapter 4 and 5 present the core part of the thesis. The formulation of IBDS and the combination of IBDS and SBM are described. Chapter 4 deals with the derivation of the formulas. Several examples of EIT forward problem are presented in Chapter 5, such as homogenous case, concentric case, Casinni oval anomaly case and multi-anomaly case.

Finally, in chapter 6, the conclusions of the thesis are given and future work is envisaged.

2. EIT forward problem

In EIT forward problem, the voltages inside the domain Ω and on the surface ∂Ω are computed with the given current injection and known conductivity distribution. First we should construct a physical model (mathematical model) to describe the problem in EIT in order to derive the forward problem in EIT, the equations which relate the current injections, voltage measurements and conductivity distributions have to be modeled. The physical model for EIT can be derived through Maxwell equations of electromagnetism (Nunez 1981, Malmivuo 1995, Doerstling 1995). In this chapter, the governing equation which describes the potential distribution of the domain and the boundary conditions needed to solve the governing equation are discussed. In this chapter various physical models used in the EIT are described. In this study, in solving the forward problem we use the CEM as a physical model, since CEM is considered to be close to real situation, efficient and accurate compared to other models (Cheng 1989, Somersalo 1992). The forward problem for CEM is formulated using finite element method (FEM) and boundary element method (BEM).

2.1 Background

The electromagnetic field in the domain $\Omega \in \Re^2$ can be described using the Maxwell's equation (Somersalo 1992, Ola 1993)

$$\nabla \times E = -\frac{\partial B}{\partial t}, \tag{2.1}$$

$$\nabla \times H = J + \frac{\partial D}{\partial t}, \tag{2.2}$$

where E is the electric field, H magnetic field, D electric displacement, B magnetic induction, and J current density.

Assuming that the domain Ω consists of linear and isotropic medium, thus we have

$$D = \varepsilon E, \tag{2.3}$$

$$B = \mu H, \tag{2.4}$$

$$J = \sigma E, \tag{2.5}$$

where ε is permittivity, μ permeability, and σ conductivity of the medium. Assuming that the injected currents are time harmonic with frequency ω, we have

$$E = \tilde{E} e^{i\omega t}, \tag{2.6}$$

$$B = \tilde{B} e^{i\omega t}. \tag{2.7}$$

Substituting equations (2.3) ~ (2.7) into equations (2.1) and (2.2), we can obtain

$$\begin{aligned} \nabla \times E &= -\frac{\partial B}{\partial t} = -\frac{\partial(\tilde{B} e^{i\omega t})}{\partial t} \\ &= -iw\tilde{B} e^{i\omega t} - \frac{e^{i\omega t}\partial(\tilde{B})}{\partial t} = -i\omega\mu H - \frac{e^{i\omega t}\partial(\tilde{B})}{\partial t}, \end{aligned} \tag{2.8}$$

$$\begin{aligned} \nabla \times H &= J + \frac{\partial D}{\partial t} = J + \frac{\partial(\varepsilon E)}{\partial t} = J + \frac{\varepsilon\partial(\tilde{E} e^{i\omega t})}{\partial t} \\ &= J + i\omega\varepsilon\tilde{E} e^{i\omega t} + \frac{\varepsilon e^{i\omega t}\partial(\tilde{E})}{\partial t} = J + i\omega\varepsilon E + \frac{\varepsilon e^{i\omega t}\partial(\tilde{E})}{\partial t}. \end{aligned} \tag{2.9}$$

The current density J can be separated into two components, *i.e.* ohmic current ($J^0 = \sigma E$) and current source (J^s). Putting the value of J and canceling out the oscillatory exponential terms, we get the following simplified Maxwell equations (Somersalo 1992, Ola 1993, Doerstling 1995)

$$\nabla \times E = -i\omega\mu H, \tag{2.10}$$

$$\nabla \times H = (\sigma + i\omega\varepsilon)E + J^s. \tag{2.11}$$

Now the electric field E can be expressed as

$$E = -\nabla u - \frac{\partial A}{\partial t}, \tag{2.12}$$

where u is electric potential and A magnetic vector potential.

In EIT, we assume static conditions, where the effect of magnetic induction which produces an induced electric field is neglected. Another assumption we make is that the capacitive effects $i\omega\varepsilon E$ in equation (2.9) can be neglected (Barber 1984, Baker 1989). Using these assumptions, the above equations can be expressed as

$$E = -\nabla u, \tag{2.13}$$

$$\nabla \times H = \sigma E + J^s. \tag{2.14}$$

Taking the divergence on both sides of equation (2.14), substituting equation (2.13) into equation (2.14), and also because there is no current source in the given frequency range in EIT, *i.e.* $J^s = 0$, we get

$$\nabla \cdot (\sigma \nabla u) = 0, \tag{2.15}$$

where $u = u(x, y)$, for $x, y \in \Omega$. The equation (2.15) is considered as the governing equation for forward problem of EIT. In order to solve the governing equation, a set of boundary conditions is required. In the next section, different kinds of boundary conditions, which related to different physical models in EIT, are presented.

2.2 Physical models in EIT

2.2.1 Continuum model

Continuum model is the most basic physical model in EIT. It assumes the entire surface as a conductor with no specific electrodes attached to the surface, with j as a continuous source current

$$j(\theta) = C\cos(k\theta), \tag{2.16}$$

where C is a constant.

2.2.2 Gap model

In gap model, it is assumed that the current density is constant over electrodes while it is assumed to be zero in the gap, *i.e.*

$$j = \begin{cases} \dfrac{I_l}{|e_l|} & x \in e_l,\ l = 1, 2, ...L \\ 0 & x \in \partial\Omega \setminus \bigcup_{l=1}^{L} e_l, \end{cases} \tag{2.17}$$

where $|e_l|$ is the area of the l th electrode, I_l is the current applied to the l th electrode e_l, and L is the number of electrodes.

2.2.3 Average-gap model

The average-gap model is based on the same boundary conditions as shown in gap model in equation (2.17). The main difference between the two models is that the gap model considers the voltage values measured at the centre of each electrode while the average-gap model considers the average value of potential at each electrode. Since both the gap model and average-gap model ignore the shunting effect as well as the contact impedance of the electrodes, they still overestimate the potential distribution inside the body (Somersalo 1992).

2.2.4 Shunt model

In shunt model, the shunting effect of the electrode is taken into account, which means that the potential on the electrode is assumed to be constant. The boundary condition, is expressed as

$$\int_{e_l} \sigma \frac{\partial u}{\partial \nu} dS = I_l \ , \ (x, y) \in e_l \ , \ l = 1, 2, \cdots, L, \tag{2.18}$$

where ν is the outward normal unit vector on the surface $\partial\Omega$. The shunting effect is described by the following condition

$$u = U_l , \ \ (x, y) \in e_l , \ \ l = 1, 2, \cdots, L , \tag{2.19}$$

where U_l is the measured voltage on the l th electrode. Since the contact impedances are still ignored in this model, it underestimates the potential distribution.

2.2.5 Complete electrode model (CEM)

The complete electrode model (CEM) takes into account the shunting effect as well as the contact impedance between the electrodes and the surface of the body. This model comprises the following boundary conditions

$$\int_{e_l} \sigma \frac{\partial u}{\partial \nu} dS = I_l , \ (x, y) \in e_l , \ l = 1, 2, \cdots, L , \tag{2.20}$$

$$\sigma \frac{\partial u}{\partial \nu} = 0 , \ (x, y) \in \partial\Omega \setminus \bigcup_{l=1}^{L} e_l . \tag{2.21}$$

The current applied through electrodes attached on the boundary of the object is given by equation (2.20) and equation (2.21) is the insulate condition where there is no current applied except on the electrode surface.

Apart from equation (2.20) and equation (2.21), we have additional condition which considers the contact impedance between the electrode and the surface of the body

$$u + z_l \sigma \frac{\partial u}{\partial \nu} = U_l, \ (x, y) \in e_l, \ \ l = 1, 2, \cdots, L, \tag{2.22}$$

where z_l is the effective contact impedance. The CEM has better approximation of the boundary voltages when compared to other models. Also, to ensure the existence and uniqueness of the solution, we impose the following conditions (Somersalo 1992)

$$\sum_{l=1}^{L} I_l = 0 \text{ and } \sum_{l=1}^{L} U_l = 0 . \tag{2.23}$$

2.3 Mathematical formulations for EIT forward problem

For the forward problem of EIT with CEM, as discussed in the previous subsection, a set of discrete electrical currents I_l ($l = 1, 2, \cdots, L$) is injected through an array of electrodes e_l ($l = 1, 2, ..., L$) attached on the circumference of the domain $\partial\Omega$ and the voltages are measured on those electrodes. Assuming, inclusions of conductivity σ_a that has a boundary ∂D occupying region D enclosed inside the domain Ω with background conductivity σ_b, as can be seen in figure 2.1.

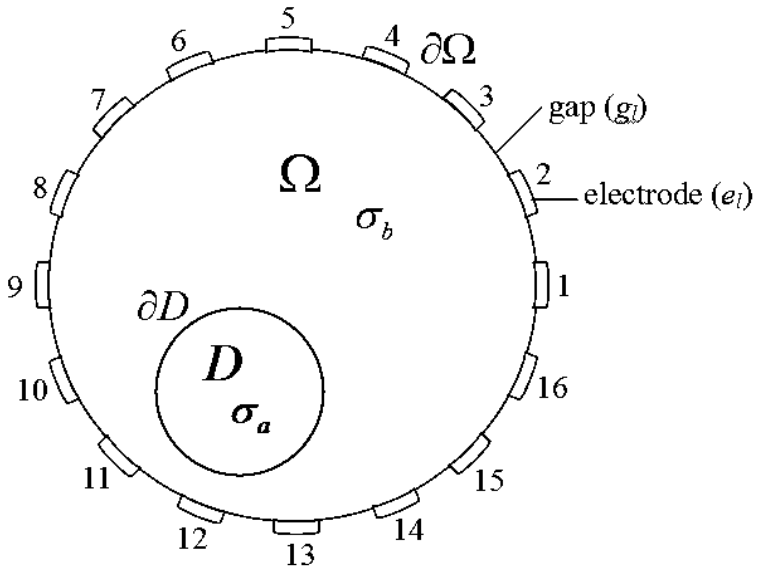

Figure 2.1. A schematic diagram of EIT domain with 16 electrodes.

The governing equation of the EIT forward problem can be expressed as

$$\nabla \cdot \left[\sigma_b + (\sigma_a - \sigma_b)\chi_D(p)\right]\nabla u(p) = 0 \quad \text{for } p \in \Omega \text{ and } D \subset \Omega, \tag{2.24}$$

subject to the boundary conditions

$$\frac{\partial u(p)}{\partial \nu} = 0 \quad \text{for } p \in \partial\Omega_G = \partial\Omega \setminus \bigcup_{l=1}^{L} e_l, \tag{2.25}$$

$$\int_{e_l} \sigma_b \frac{\partial u\ (p)}{\partial \nu} dS = I_l \quad \text{for } p \in e_l,\ l = 1, 2, \cdots, L, \tag{2.26}$$

$$u(p) + z_l \sigma_b \frac{\partial u\ (p)}{\partial \nu} = U_l \quad \text{for } p \in e_l,\ l = 1, 2, \cdots, L\ , \tag{2.27}$$

and interfacial conditions

$$u(p)\big|_{\partial D^-} = u(p)\big|_{\partial D^+} \text{ and } \sigma_a \frac{\partial u(p)}{\partial \nu}\bigg|_{\partial D^-} = \sigma_b \frac{\partial u(p)}{\partial \nu}\bigg|_{\partial D^+}, \tag{2.28}$$

where $\chi_D(p) = 1$ if p located in D, otherwise $\chi_D(p) = 0$, $\partial\Omega = \partial\Omega_G \bigcup \partial\Omega_E$, $\partial\Omega_E = \bigcup_{l=1}^{L} e_l$, and $\partial\Omega_G = \bigcup_{l=1}^{L} g_l$.

Or, the governing equation can be expressed as

$$\nabla^2 u_b(p) = 0 \text{ for } p \in \Omega \setminus \bar{D}, \tag{2.29}$$

$$\nabla^2 u_a(p) = 0 \text{ for } p \in D, \tag{2.30}$$

subject to the boundary conditions

$$\frac{\partial u_b(p)}{\partial \nu} = 0 \text{ for } p \in \partial\Omega_G = \partial\Omega \setminus \bigcup_{l=1}^{L} e_l, \tag{2.31}$$

$$\int_{e_l} \sigma_b \frac{\partial u_b(p)}{\partial \nu} dS = I_l \quad \text{for } p \in e_l,\ l = 1, 2, \cdots, L, \tag{2.32}$$

$$u_b(p) + z_l \sigma_b \frac{\partial u_b(p)}{\partial \nu} = U_l \quad \text{for } p \in e_l,\ l = 1, 2, \cdots, L, \tag{2.33}$$

and interfacial conditions,

$$u_a(p)\big|_{\partial D^-} = u_b(p)\big|_{\partial D^+} \text{ and } \sigma_a \frac{\partial u_a(p)}{\partial \nu}\bigg|_{\partial D^-} = \sigma_b \frac{\partial u_b(p)}{\partial \nu}\bigg|_{\partial D^+}. \tag{2.34}$$

Also, the current and the potentials should satisfy the constraints as described in equation (2.23).

2.3.1 Finite element method formulation of EIT

In the FEM implementation of EIT forward problem described in the previous subsection, the object Ω is discretized into small triangular elements (Vauhkonen

1997, Khampampati 2010). We assume that the resistivity is uniform within each element. Suppose the number of nodes in the finite element mesh is *N*, then the potential distribution u within the object can be approximated as

$$u \approx u^h(p) = u^h(x, y) = \sum_{i=1}^{N} \alpha_i \varphi_i(x, y), \tag{2.35}$$

and the potential on the electrodes is represented as

$$U^h = \sum_{j=1}^{L-1} \beta_j \mathbf{n}_j, \tag{2.36}$$

where ϕ_i is two-dimensional first-order basis function, α_i and β_i are the coefficients to be determined, and $\mathbf{n}_j$ are the bases for the measurements, is the *j*th column of matrix $\mathbf{n}$, and

$$\mathbf{n} = \begin{bmatrix} 1 & 1 & \cdots & 1 \\ -1 & 0 & \cdots & 0 \\ 0 & -1 & \cdots & 0 \\ \vdots & \vdots & \ddots & \vdots \\ 0 & 0 & \cdots & -1 \end{bmatrix} \in \Re^{L\times(L-1)}, \tag{2.37}$$

i.e.

$$\mathbf{n}_1 = (1, -1, 0, \cdots, 0)^T$$
$$\mathbf{n}_2 = (1, 0, -1, 0, \cdots, 0)^T \in \Re^L .$$
$$\vdots$$

The finite element formulation gives the following system of linear equations

$$\mathbf{Ab} = \tilde{\mathbf{I}}, \tag{2.38}$$

where

$$\mathbf{A}=\begin{pmatrix}\mathbf{B} & \mathbf{C}\\ \mathbf{C}^T & \mathbf{D}\end{pmatrix},\qquad \mathbf{b}=\begin{pmatrix}\boldsymbol{\alpha}\\ \boldsymbol{\beta}\end{pmatrix}\ \text{and}\ \ \tilde{\mathbf{I}}=\begin{pmatrix}\mathbf{0}\\ \boldsymbol{\zeta}\end{pmatrix}, \tag{2.39}$$

$\boldsymbol{\alpha}=(\alpha_1,\alpha_2,\cdots,\alpha_N)^T\in\Re^N$,

$\boldsymbol{\beta}=(\beta_1,\beta_2,\cdots,\beta_{L-1})^T\in\Re^{L-1}$,

$\mathbf{0}\in\Re^N$, and

$\boldsymbol{\zeta}=(I_1-I_2,I_1-I_3,\cdots,I_1-I_L)^T\in\Re^{L-1}$.

and the stiffness matrix $\mathbf{A}$ is of the form

$$\mathbf{B}(i,j)=\int_\Omega \sigma\nabla\varphi_i\cdot\nabla\varphi_j d\Omega+\sum_{\ell=1}^{L}\frac{1}{z_\ell}\int_{e_l}\varphi_i\varphi_j dS\ ,\ \text{for}\ \ i,j=1,2,\cdots,N\ , \tag{2.40}$$

$$\mathbf{C}(i,j)=-\frac{1}{z_1}\int_{e_1}\varphi_i dS+\frac{1}{z_{j+1}}\int_{e_{j+1}}\varphi_i dS\ ,\ \text{for}\ \ i=1,2,\cdots,N\ ,\ \ j=1,2,\cdots,L-1\ , \tag{2.41}$$

$$\mathbf{D}(i,j)=\begin{cases}\dfrac{|e_1|}{z_1} & i\neq j\\ \dfrac{|e_1|}{z_1}+\dfrac{|e_{j+1}|}{z_{j+1}} & i=j\end{cases},\ \text{for}\ \ i,j=1,2,\cdots,L-1, \tag{2.42}$$

where $|e_j|$ is the area of the electrode j.

In some cases, the voltages are measured only at some selected electrodes, not every electrode. Also, the selected electrodes may be different at each current pattern. The measured voltages at the measurement electrodes $\hat{\mathbf{U}}$ can be obtained as

$$\hat{\mathbf{U}}=\mathbf{M}^T\mathbf{U}^h=\mathbf{M}^T\mathbf{N}\boldsymbol{\beta}\in\Re^{E\times P}, \tag{2.43}$$

where, E is the number of the measurement electrodes, P is the number of current patterns and $\mathbf{M} \in \Re^{L \times E}$ is the measurement matrix. Furthermore, $\mathbf{U}^h$ can be extracted directly from $\mathbf{b}$ by introducing the extended mapping matrix $\tilde{\mathbf{N}}$

$$\tilde{\mathbf{N}} = (\mathbf{0}, \mathbf{N}) \in \Re^{L \times (N+L-1)} \text{ and } \mathbf{U}^h = \tilde{\mathbf{N}}\mathbf{b}, \tag{2.44}$$

where $\mathbf{0} \in \Re^{L \times N}$. Therefore, we have

$$\hat{\mathbf{U}} = \mathbf{M}^T \mathbf{U}^h = \mathbf{M}^T \tilde{\mathbf{N}}\mathbf{b} = \tilde{\mathbf{M}}\mathbf{b}, \tag{2.45}$$

where the extended measurement matrix is defined as

$$\tilde{\mathbf{M}} = \mathbf{M}^T \tilde{\mathbf{N}} \in \Re^{E \times (N+L-1)}. \tag{2.46}$$

2.3.2 Boundary element method formulation of EIT

The boundary element method formulation (Duraiswami 1997, de Munck 2000, Khampampati 2011, Khampampati 2012) is based on the fundamental solution of the Laplace equation. Here, we denote the fundamental solution of Laplace equation by *G*, so that

$$\Delta_p G(p \mid p_s) = \delta(p - p_s), \tag{2.47}$$

where p is the field point, p_s the source point.

The solution of Laplace equation *G* and its normal derivative *Q* in 2D are

$$G(p \mid p_s) = \frac{1}{4\pi} \ln \left| p_s - p \right|^2 = \frac{1}{4\pi} \ln r^2, \tag{2.48}$$

$$Q(p \mid p_s) = \frac{\partial}{\partial \nu} G(p \mid p_s)$$
$$= -\frac{1}{2\pi} \frac{(p_s - p) \cdot \nu(p)}{|p_s - p|^2} = -\frac{1}{2\pi} \frac{(p_s - p) \cdot \nu(p)}{r^2}, \tag{2.49}$$

where $r = |p_s - p|$.

From (2.29), (2.30), and (2.23), and using Greens second identity, we have

$$\int_{\partial\Omega} G(p \mid p_s) \frac{\partial u_b(p)}{\partial \nu} dS + \int_{\partial D} G(p \mid p_s) \frac{\partial u_b(p)}{\partial \nu} dS - \int_{\Omega \setminus \bar{D}} \nabla u_b(p) \cdot \nabla G(p \mid p_s) d\Omega = 0, \tag{2.50}$$

$$\int_{\partial D} G(p \mid p_s) \frac{\partial u_a(p)}{\partial \nu} dS - \int_{D} \nabla u_a(p) \cdot \nabla G(p \mid p_s) d\Omega = 0, \tag{2.51}$$

by using

$$\int_{\Omega \setminus \bar{D}} G(p \mid p_s) \nabla^2 u_b(p) d\Omega = 0, \tag{2.52}$$

$$\int_{D} G(p \mid p_s) \nabla^2 u_a(p) d\Omega = 0. \tag{2.53}$$

Applying the Gauss theorem and substituting equation (2.50) and equation (2.51), we can obtain

$$\int_{\Omega \setminus \bar{D}} u_b(p) \nabla^2 G(p \mid p_s) d\Omega = \int_{\Omega \setminus \bar{D}} u_b(p) \delta(p - p_s) d\Omega, \tag{2.54}$$

$$\int_{D} u_a(p) \nabla^2 G(p \mid p_s) d\Omega = \int_{D} u_a(p) \delta(p - p_s) d\Omega, \tag{2.55}$$

$$\int_{\Omega \setminus \bar{D}} u_b(p) \nabla^2 G(p \mid p_s) d\Omega$$
$$= \int_{\partial\Omega} u_b(p) Q(p \mid p_s) dS + \int_{\partial D} u_b(p) Q(p \mid p_s) dS - \int_{\Omega \setminus \bar{D}} \nabla u_b(p) \cdot \nabla G(p \mid p_s) d\Omega,$$

(2.56)

$$\int_{\Omega\setminus\bar{D}} u_b(p)\delta(p-p_s)d\Omega = \omega_b(p_s)u_b(p_s), \quad \text{for } p_s \in \bar{\Omega}\setminus D \tag{2.57}$$

$$\int_D u_a(p)\nabla^2 G(p\,|\,p_s)d\Omega = \int_{\partial D} u_a(p)Q(p\,|\,p_s)dS - \int_D \nabla u_a(p)\cdot\nabla G(p\,|\,p_s)d\Omega\ ,$$

(2.58)

$$\int_D u_a(p)\delta(p-p_s)d\Omega = \omega_a(p_s)u_a(p_s)\ , \quad \text{for } p_s \in \bar{D} \tag{2.59}$$

here, ω_b and ω_a are the geometric coefficients on the boundaries. The geometric coefficient is computed by the internal angle at the point divided by 2π.

Define

$$q(p) = \frac{\partial u(p)}{\partial \nu}, \tag{2.60}$$

we have the identities:

$$\begin{aligned}\omega_b(p_s)u_b(p_s) = &\int_{\partial\Omega} u_b(p)Q(p,p_s)dS + \int_{\partial D} u_b(p)Q(p,p_s)dS \\ &- \int_{\partial\Omega} q_b(p)G(p,p_s)\frac{\partial u_b(p)}{\partial \nu}dS - \int_{\partial D} q_b(p)G(p,p_s)dS\end{aligned}\ , \tag{2.61}$$

$$\omega_a(p_s)u_a(p_s) = \int_{\partial D} u_a(p)Q(p\,|\,p_s)dS - \int_{\partial D} q_a(p)G(p\,|\,p_s)dS\,, \tag{2.62}$$

From the interfacial conditions

$$u_a(p)\big|_{\partial D^-} = u_b(p)\big|_{\partial D^+}, \tag{2.63}$$

and

$$-\kappa q_a(p)\big|_{\partial D^-} = q_b(p)\big|_{\partial D^+}, \tag{2.64}$$

where $\kappa = \sigma_a / \sigma_b$. Note that the outward unit normal vector on ∂D^- is opposed to that on ∂D^+. Hence, from the above representation formulas becomes

$$\begin{aligned}
&\left[\omega_b(p_s) + \kappa\omega_a(p_s)\chi_{\partial D}(p_s)\right]u_b(p_s) \\
&= \int_{\partial\Omega} u_b(p)Q(p \mid p_s)dS - \int_{\partial\Omega} q_b(p)G(p \mid p_s)dS \quad , \qquad \text{for } p_s \in \bar{\Omega} \setminus D \\
&\quad +(1-\kappa)\int_{\partial D} u_b(p)Q(p \mid p_s)dS
\end{aligned} \tag{2.65}$$

and

$$\begin{aligned}
&\left[\omega_b(p_s) + \kappa\omega_a(p_s)\chi_{\partial D}(p_s)\right]u_b(p_s) \\
&= \int_{\partial\Omega} u_b(p)Q(p \mid p_s)dS - \sum_{l=1}^{L}\int_{e_l} \frac{U_l - u_b(p)}{z_l\sigma_b} G(p \mid p_s)dS + (1-\kappa)\int_{\partial D} u_b(p)Q(p \mid p_s)dS \\
&= \int_{\partial\Omega} u_b(p)Q(p \mid p_s)dS + \sum_{l=1}^{L}\frac{1}{z_l\sigma_b}\int_{e_l} u_b(p)G(p \mid p_s)dS + (1-\kappa)\int_{\partial D} u_b(p)Q(p \mid p_s)dS \,, \\
&\quad -\sum_{l=1}^{L}\frac{U_l}{z_l\sigma_b}\int_{e_l} G(p \mid p_s)dS
\end{aligned} \tag{2.66}$$

for $p_s \in \bar{\Omega} \setminus D$.

The above representation formulas can be rewritten as

$$\begin{aligned}
\omega(p_s)u_b(p_s) = &\int_{\partial\Omega} u_b(p)Q(p \mid p_s)dS + \sum_{l=1}^{L}\frac{1}{z_l\sigma_b}\int_{e_l} u_b(p)G(p \mid p_s)dS \\
&+(1-\kappa)\int_{\partial D} u_b(p)Q(p \mid p_s)dS - \sum_{l=1}^{L}\frac{U_l}{z_l\sigma_b}\int_{e_l} G(p \mid p_s)dS
\end{aligned} \,, \tag{2.67}$$

for $p_s \in \bar{\Omega} \setminus D$, and

$$\frac{1}{|e_l|}\int_{e_l} u(p)dS + \frac{z_l I_l}{|e_l|} = U_l \quad \text{for} \quad l = 1, 2, \cdots, L \,, \tag{2.68}$$

where

$$\omega(p_s) = \omega_b(p_s) + \kappa\omega_a(p_s)\chi_{\partial D}(p_s)\,. \tag{2.69}$$

Assume that the electrodes are spaced equally on the boundary and has the same size of $|e|$. Each electrode and each gap regions are uniformly discretized into m_E and m_G segments, respectively. Hence, the total numbers of the electrode and the gap segments are $M_E = Lm_E$ and $M_G = Lm_G$, respectively. The i th segment of the electrode region is denoted by $\partial\Omega_{E_i}$ ($i = 1,2,\cdots,M_E$) and by the same way, $\partial\Omega_{G_i}$ ($i = 1,2,\cdots,M_E$) stands for the i th segment of the gap region. The sizes of the electrode and gap segments are set to s_E and s_G. If the number of the segments of the inclusion boundaries is M_D, the total number of segments is $M = M_E + M_G + M_D$.

The discretized form will be

$$D(\omega)\begin{bmatrix} u_E \\ u_G \\ u_D \end{bmatrix} - \begin{bmatrix} K_E & K_G & (1-\kappa)K_D \end{bmatrix}\begin{bmatrix} u_E \\ u_G \\ u_D \end{bmatrix} + K_U U = 0\,, \tag{2.70}$$

$$U = Au_E + D(z_l / |e_l|)\tilde{I}\,, \tag{2.71}$$

where

$$D(\omega) = \mathrm{diag}\begin{bmatrix} \omega(p_1) & \omega(p_2) & \cdots & \omega(p_M) \end{bmatrix} \in \Re^{M\times M}\,, \tag{2.72}$$

$$Q_E(i,j) = \int_{\partial\Omega_{E_j}} Q(p \mid p_i)dS \in \Re^{M\times M_E}\,, \tag{2.73}$$

$$G_E(i,j) = \int_{\partial\Omega_{E_j}} G(p \mid p_i)dS \in \Re^{M\times M_E}\,, \tag{2.74}$$

$$K_E = Q_E + \frac{1}{\sigma_b} G_E \left[D(1/z_l) \otimes I_{m_E} \right] \in \Re^{M \times M_E} \ , \tag{2.75}$$

$$K_G(i,j) = \int_{\partial \Omega_{G_j}} Q(p \mid p_i) dS \in \Re^{M \times M_G} , \tag{2.76}$$

$$K_D(i,j) = \int_{\partial D_j} Q(p \mid p_i) dS \in \Re^{M \times M_D} \ , \tag{2.77}$$

$$K_U(i,l) = \frac{1}{z_l \sigma_b} \int_{e_l} G(p \mid p_i) dS \in \Re^{M \times L} \ , \tag{2.78}$$

or

$$K_U = \frac{1}{\sigma_b} G_E \left[D(1/z_l) \otimes \text{ones}(m_E, 1) \right] \in \Re^{M \times L} \ , \tag{2.79}$$

$$U = \begin{bmatrix} U_1 & U_2 & \cdots & U_L \end{bmatrix}^T \ , \tag{2.80}$$

$$A = \frac{s_E}{|e|} I_L \otimes \text{ones}(1, m_E) \in \Re^{L \times M_E} , \tag{2.81}$$

$$D(z_l / |e_l|) = \text{diag}\left[z_1 / |e_1| \quad z_2 / |e_2| \quad \cdots \quad z_L / |e_L| \right]. \tag{2.82}$$

In this, $\otimes$ denotes the Kronecker matrix product, $I_{M_E} \in \Re^{M_E \times M_E}$ the identity matrix, and ones(m,n) the m-by-n matrix with ones. In order to satisfy the constraint $\sum_{l=1}^{L} U_l = 0$, let's define

$$U = \begin{pmatrix} U_1 \\ U_2 \\ U_3 \\ \vdots \\ U_L \end{pmatrix} = N_U \beta = \begin{pmatrix} 1 & 1 & \cdots & 1 \\ -1 & 0 & \cdots & 0 \\ 0 & -1 & \cdots & 0 \\ \vdots & \vdots & \ddots & \vdots \\ 0 & 0 & \cdots & -1 \end{pmatrix} \begin{pmatrix} \beta_1 \\ \beta_2 \\ \beta_3 \\ \vdots \\ \beta_{L-1} \end{pmatrix} = \begin{pmatrix} \beta_1 + \beta_2 + \cdots + \beta_{L-1} \\ -\beta_1 \\ -\beta_2 \\ \vdots \\ -\beta_{L-1} \end{pmatrix} , \tag{2.83}$$

where

$$N_U = \left[\text{ones}(1, L-1); -I_{L-1}\right] . \tag{2.84}$$

Then,

$$D(\omega)\begin{bmatrix} u_E \\ u_G \\ u_D \end{bmatrix} - \begin{bmatrix} K_E & K_G & (1-\kappa)K_D \end{bmatrix}\begin{bmatrix} u_E \\ u_G \\ u_D \end{bmatrix} + K_U N_U \beta = 0, \tag{2.85}$$

$$N_U \beta = A u_E + D(z_l / |e_l|)\tilde{I} \ , \tag{2.86}$$

$$\beta = \left[N_U^T N_U\right]^{-1} N_U^T \left[A u_E + D(z_l / |e_l|)\tilde{I}\right], \tag{2.87}$$

$$\begin{aligned} &D(\omega)\begin{bmatrix} u_E \\ u_G \\ u_D \end{bmatrix} - \begin{bmatrix} K_E & K_G & (1-\kappa)K_D \end{bmatrix}\begin{bmatrix} u_E \\ u_G \\ u_D \end{bmatrix} \\ &+ K_U N_U \left[N_U^T N_U\right]^{-1} N_U^T \left[A u_E + D(z_l / |e_l|)\tilde{I}\right] = 0 \end{aligned} \quad . \tag{2.88}$$

Finally, we have

$$\left[D(\omega) - \left[K_E - K_U \tilde{N} A \quad K_G \quad (1-\kappa)K_D\right]\right]\begin{bmatrix} u_E \\ u_G \\ u_D \end{bmatrix} = -K_U \tilde{N} D(z_l / |e_l|)\tilde{I} \ , \tag{2.89}$$

where

$$\tilde{N} = N_U \left[N_U^T N_U\right]^{-1} N_U^T . \tag{2.90}$$

Consider the m th boundary dS_m where a local point p is contained and dS_m is approximated to a linear segment of length l_m.

$$p = p_0 + \frac{t}{2}(p_2 - p_1), \tag{2.91}$$

where the end points p_1 and p_2 are numbered counterclockwise on $\partial\Omega$ and clockwise on ∂D.

$$dS_m = \sqrt{(dx/dt)^2 + (dy/dt)^2}\,dt = \frac{l_m}{2}dt\,, \tag{2.92}$$

$$\begin{aligned} r^2 &= (x-x_s)^2 + (y-y_s)^2 = \left[x_0 + \frac{t}{2}(x_2 - x_1) - x_s\right]^2 + \left[y_0 + \frac{t}{2}(y_2 - y_1) - y_s\right]^2 \\ &= (x_0 - x_s)^2 + (y_0 - y_s)^2 + \left[(x_0 - x_s)(x_2 - x_1) + (y_0 - y_s)(y_2 - y_1)\right]t \\ &+ \left[(x_2 - x_1)^2 + (y_2 - y_1)^2\right]\frac{t^2}{4} \\ &= \left|p_0 - p_s\right|^2 + (p_0 - p_s)\cdot(p_2 - p_1)t + \left|p_2 - p_1\right|^2\frac{t^2}{4} \\ &= a + bt + ct^2 \\ &= c\left(t + \frac{b}{2c}\right)^2 + \frac{4ac - b^2}{4c} \end{aligned} \tag{2.93}$$

where

$$a = \left|p_0 - p_s\right|^2 \geq 0\,,$$

$$b = (p_0 - p_s)\cdot(p_2 - p_1)\,,$$

$$c = \frac{1}{4}\left|p_2 - p_1\right|^2 > 0\,.$$

The discriminate is

$$\begin{aligned} d^2 = 4ac - b^2 &= \left|p_0 - p_s\right|^2\left|p_2 - p_1\right|^2(1 - \cos^2\theta) = \left|p_0 - p_s\right|^2\left|p_2 - p_1\right|^2\sin^2\theta \\ &= \left|(p_0 - p_s)\times(p_2 - p_1)\right|^2 \end{aligned}\,. \tag{2.94}$$

Thus,

$$G(p \mid p_s) = \frac{1}{2\pi}\ln\left|p - p_s\right| = \frac{1}{4\pi}\ln\left|p - p_s\right|^2 = \frac{1}{4\pi}\ln r^2 = \frac{1}{4\pi}\ln(a + bt + ct^2)\,, \tag{2.95}$$

$$Q(p \mid p_s) = \frac{\partial G(p \mid p_s)}{\partial \nu} = \frac{(p - p_s)\cdot\nu}{2\pi\left|p - p_s\right|^2} = \frac{(p - p_s)\cdot\nu}{2\pi r^2} = \frac{(p - p_s)\cdot(p_2 - p_1)^{\perp}}{2\pi l_m(a + bt + ct^2)}\,, \tag{2.96}$$

since

$$
\begin{aligned}
&(p-p_s)\cdot(p_2-p_1)^{\perp}=(x-x_s)(y_2-y_1)-(y-y_s)(x_2-x_1)=(p-p_s)\times(p_2-p_1)\cdot\hat{k}\\
&=\left[(x_0-x_s)+\frac{t}{2}(x_2-x_1)\right](y_2-y_1)-\left[(y_0-y_s)+\frac{t}{2}(y_2-y_1)\right](x_2-x_1)\\
&=(x_0-x_s)(y_2-y_1)-(y_0-y_s)(x_2-x_1)=(p_0-p_s)\times(p_2-p_1)\cdot\hat{k}
\end{aligned}
\qquad (2.97)
$$

we can rewrite equation (2.97) as

$$
Q(p\mid p_s)=\frac{\partial G(p\mid p_s)}{\partial \nu}=\frac{(p_0-p_s)\times(p_2-p_1)\cdot\hat{k}}{2\pi l_m(a+bt+ct^2)}=\frac{d}{2\pi l_m(a+bt+ct^2)}, \qquad (2.98)
$$

where $d=(p_0-p_s)\times(p_2-p_1)\cdot\hat{k}$.

Finally, we can have

$$
\begin{aligned}
Q(p_m,p_s)&=\int_{S_m}Q(p\mid p_s)dS\\
&=\begin{cases}\dfrac{sign(d)}{2\pi}\left(\tan^{-1}\dfrac{b+2c}{|d|}-\tan^{-1}\dfrac{b-2c}{|d|}\right) & for \quad |d|>0\\ 0 \quad for \quad |d|=0\end{cases}
\end{aligned}
\qquad (2.99)
$$

and

$$
\begin{aligned}
&G(p_m,p_s)=\int_{S_m}G(p\mid p_s)dS=\frac{l_m}{8\pi}\int_{-1}^{1}\ln(a+bt+ct^2)dt\\
&=\frac{l_m}{8\pi}\left[\left(1+\frac{b}{2c}\right)\ln(a+b+c)+\left(1-\frac{b}{2c}\right)\ln(a-b+c)-4\right]+\frac{l_m d}{4c}Q(p_m,p_s)
\end{aligned}
\qquad (2.100)
$$

Once all the coefficients of equation (2.89) are determined, the potential at any point on the boundary can be evaluated by solving equation (2.89).

3. Method of fundamental solutions (MFS)

Among the MMs, the method of fundamental solutions (MFS) has gained an increasing attention in many engineering and science fields (Mathon 1977, Rek 1999, Young 2005, Young 2006, Sarler 2009, Chen 2006, Chen 2012). The MFS is the first kind of boundary-type discretization MMs (Karageorghis 1992, Fairwaether 1998, Chen 1998, Liu 2005, Young 2005). In order to avoid the singularity of fundamental solutions with a strong-form collocation formulation, the MFS places the source points on a fictitious boundary outside or inside the physical domain, corresponding to interior or exterior problems, respectively. MFS is effective for solving the elliptic well-posed direct problems in complex geometries (Shigeta 2009, Young 2005, Young 2006, Chen 2006, Chen 2010, Chen 2012). Mathon and Johnston (Mathon 1977) first showed numerical results obtained by using the MFS. The papers Bogomolny (1985), Katsurada (1996), Sarler (2009) and Liu (2010) had discussed some mathematical theories regarding the MFS.

MFS has been used to solve the Laplace equation (Bogomolny 1985, Fairweather 1998, Saavedra 2003). The error estimates, stability and convergence analyses of the MFS for the Laplace equation in a circular domain are carried out by Bogomolny (1985), and Smyrlis and Karageorghis (2001). The MFS has a wide application in engineering fields, examples can be seen in Chio *et al.* (2004), Young *et al.* (2005), Young and Ruan (2005), Chen *et al.* (2008), and Liu (2011). Fairweather (1998) and Karageorghis *et al.* (2011) had given a comprehensive review regarding the applications of MFS to the linear inverse problems.

The MFS is very easy to numerically implement and it can avoid the integrations on the boundary. However the MFS has a serious disadvantage that the resulting linear equations system may become highly ill-conditioned when the number of source points is increased (Young 2005, Chen 2006, Liu 2012) or when the distances of source points are increased (Chen 2006). The convergence analysis of MFS has demonstrated that the approximation improves when the source radius

tends to infinity as reported by Smyrlis and Karageorghis (2004). Nevertheless, for complex geometries, the MFS also requires large number of nodes to collocate the boundary conditions, and in general it gives a better accuracy than that only using a small number of nodes on the boundary. Besides, it is also known that the MFS may produces some difficulties while dealing with complicated geometries with discontinuous boundary conditions, which require special treatment by using the technique of enrichment functions which was proposed by Alves and Leitao (2006).

Tsai *et al.* (2006) have proposed a numerical procedure to locate the source points of the MFS. They proposed a practical procedure to locate the source points in the use of MFS for various time independent operators. The location procedure was developed through some systematically numerical experiments for the relations among the accuracy, condition number, and location of source points in different shapes of computational domains. By numerical experiments, they found that good accuracy could be achieved when the condition number approaches the limit of equation solver. In their numerical experiments, higher condition numbers and smaller errors were obtained when the source points are located farther in some proper way.

By using the super-singular double-layer fundamental solution, an alternative collocation strong-form method, called the modified method of fundamental solution (MMFS), was proposed by Young and his coworkers (Young 2005, Young 2006, Chen 2006, Young 2007). The troublesome singularity was avoided by employing the subtracting and adding-back techniques without a fictitious boundary as contrasted to the conventional MFS. Therefore, the major difficulty of the coincidence of the source points and collocation points in the conventional MFS is thereby overcame. The method had been further extended to the single layer Laplace equation fundamental solution in by Young *et al.* (2006). Sarler (2009) applied the MMFS to potential flow problems. The solution in two-dimensional Cartesian coordinates was represented in terms of the single layer and the double layer fundamental solutions. The desingularisation technique was put into the context of potential flow problems by using and comparing the single layer fundamental

solution (SLFS) and the double layer fundamental solution (DLFS). The calculation of the desingularised values of the partial derivatives on the boundary was represented as well, which was different from the case in the previous two cited MMFS pioneering papers by Young's group. Based on the MMFS, the regularized meshless method (RMM) (Chen 2006) was developed to solve two-dimensional Laplace problem with multiply-connected geometries. The approximate solution was represented by using the double-layer fundamental solution. The source points was located on the physical boundary as well as the MMFS by using the proposed technique to regularize the singularity of the kernel functions.

Liu (2010) proposed a boundary distributed source (BDS) method, in which the fundamental solution was integrated over small areas covering the source points so that the fictitious boundary was avoided and the coefficients in the system equations could be evaluated analytically. However, the analytical expression of the diagonal elements for equations describe the Neumann boundary condition had to be determined in a indirect way. And thus this method is still immature and under further developments (Perne 2012).

The singular boundary meshless method (SBM), proposed by Chen and his collaborators (Chen 2009a, Chen 2009b, Chen 2010, Gu 2011, Chen 2012) overcame the artificial boundary in the conventional MFS by locating the source point to coincide with the collocation points on the physical boundary. The key idea of SBM was to introduce the concept of the origin intensity factor to isolate the singularity of the fundamental solution. And an inverse interpolation technique was proposed to evaluate the origin intensity factor. However, in order to carry out this technique, the SBM had to place a cluster of sample nodes inside or outside the physical domain for either interior or exterior problems. Chen *et al.* (2012) indicated that the solution accuracy of this SBM formulation was sensitive to the placement of such sample nodes. They developed a novel formulation of the SBM to avoid the above-mentioned sample nodes in the ordinary SBM formulation, based on the subtracting and adding-back technique as well as the inverse interpolation technique. The new formulation circumvented the major shortcomings in the ordinary SBM while

retaining its advantages such as being mathematically simple, easy to program, high accuracy, and free from integration.

In this section, the conventional MFS, MMFS, RMM, BDS and SBM are briefly reviewed and the main formulations of the MMs are presented.

3.1 Conventional method of fundamental solution (MFS)

The MFS (Karageorghis 1992, Fairwaether 1998, Chen 1998, Liu 2005, Shigeta 2009) based on the fundamental solution of a partial differential equation of interest, is compromised by requiring a controversial fictitious boundary outside the physical domain to refrain from the singularity of fundamental solution. The approximate solution in MFS is a linear combination of fundamental solutions, which automatically satisfy the governing equation. The coefficients used in the linear combination are determined from the given boundary conditions.

Consider the Laplace equation

$$\Delta u = 0, \tag{3.1}$$

in a two-dimensional bounded domain Ω enclosed by the boundary $\partial\Omega$. We prescribe Dirichlet and Neumann boundary conditions on a part of the boundary $\partial\Omega$, denoted by $\partial\Omega_1$ and $\partial\Omega_2$, as follows

$$u = \overline{u} \quad \text{on} \quad \partial\Omega_1, \tag{3.2}$$

$$\frac{\partial u}{\partial \nu} = \overline{q} \quad \text{on} \quad \partial\Omega_2, \tag{3.3}$$

where $\overline{u}$ and $\overline{q}$ denote given continuous functions defined on $\partial\Omega$, and ν the unit outward normal to $\partial\Omega$. Then, we need to find the boundary value u on the rest of the boundary $\partial\Omega_2 = \partial\Omega \setminus \partial\Omega_1$ or the potential u in the domain Ω.

The fundamental solution of the Laplace equation in two dimensions is defined as

$$\varphi^*(r) = -\frac{1}{2\pi}\ln r\,, \tag{3.4}$$

where $r = |\mathrm{x}| = \sqrt{x^2 + y^2}$, which is a solution to

$$\Delta\phi^* = \delta(\mathrm{x})\,, \tag{3.5}$$

where δ denotes Dirac delta function.

We distribute the collocation (field) points $\{\mathrm{x}_i\}_{i=1}^{M} \subset \partial\Omega$ on the boundary, and the source points $\{s_j\}_{j=1}^{N} \subset \bar{\Omega}^c$ on a fictitious boundary outside the domain. Generally, there are two ways to locate the source points, one is distributed the source points on a circle outside the domain (Tsai 2006, Shigeta 2009), as shown in figure 3.1. Another way is to distribute the source point outside the domain with a certain distance from each collocation points, as shown in figure 3.2.

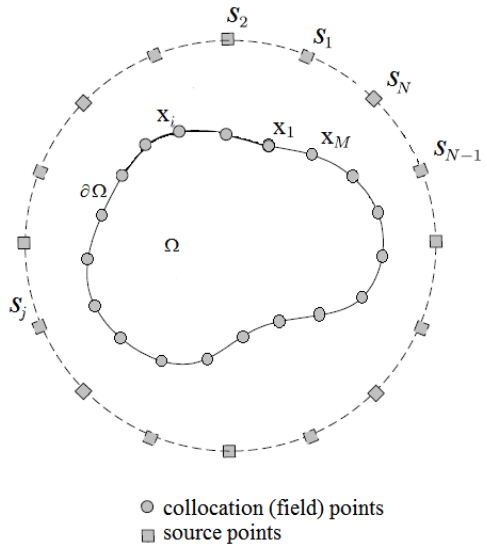

Figure 3.1. Schematic diagram which explains the node distribution in MFS.

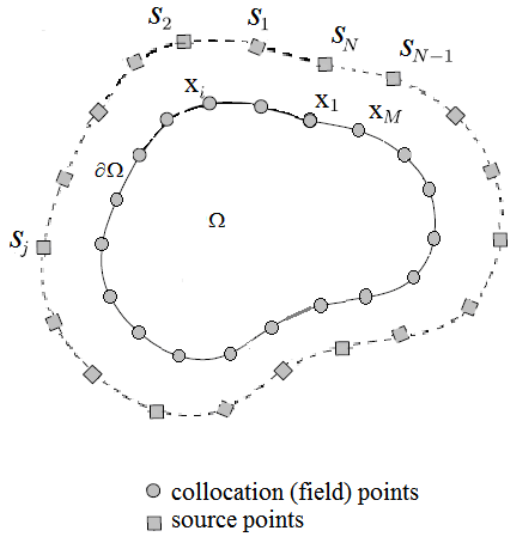

Figure 3.2. Schematic diagram which explains the node distribution in conventional MFS.

The approximate solution is expressed as a linear combination of fundamental solutions

$$u(\mathrm{x}) \approx u_N(\mathrm{x}) = \sum_{j=1}^{N} w_j \phi_j(\mathrm{x}), \tag{3.6}$$

where the basis function is defined as

$$\phi_j(\mathrm{x}) = \phi^*(|\mathrm{x}-s_j|), \tag{3.7}$$

and $\{w_j\}_{j=1}^{N}$ are unknown coefficients which need to determined by using the boundary conditions. Since the basis functions (3.7) have no singular points in Ω, the approximate function u_N satisfies the Laplace equation (3.1). Substituting equation (3.6) into equations (3.2) and (3.3), assuming that equations (3.2) and (3.3) is satisfied at the collocation points, we have

$$\sum_{j=1}^{N} w_j \phi_j(\mathrm{x}) = \overline{u}(\mathrm{x}_i) \quad \text{for } i = 1,\ 2,\ ....,\ M\,, \tag{3.8}$$

$$\sum_{j=1}^{N} w_j \frac{\partial \phi_j(\mathrm{x})}{\partial \nu} = \overline{q}(\mathrm{x}_i) \quad \text{for } i = 1,\ 2,\ ....,\ M\,. \tag{3.9}$$

Or in matrix form

$$\mathrm{A}\boldsymbol{w} = \boldsymbol{b}, \tag{3.10}$$

where $\mathrm{A} = (a_{ij}) \in \Re^{2M \times N}$ and the vectors $\boldsymbol{w} = (w_j) \in \Re^{N}, \boldsymbol{b} = (b_i) \in \Re^{2M}$ are defined by

$$a_{ij} = \begin{cases} \phi_j(\mathrm{x}_i), & i = 1,\ 2,\ ....,M, \text{ and } j = 1,\ 2,\ ....,N \\ \dfrac{\partial \phi_j(\mathrm{x}_{i-M})}{\partial \nu}, & i = M+1,\ M+2,\ ....,2M, \text{ and } j = 1,\ 2,\ ....,N \end{cases}, \tag{3.11}$$

$$b_i = \begin{cases} \overline{u}(\mathrm{x}_i), & i = 1,\ 2,\ ....,M \\ \overline{q}(\mathrm{x}_{i-M}), & i = M+1,\ M+2,\ ....,2M \end{cases}. \tag{3.12}$$

3.2 Modified method of fundamental solution (MMFS)

The Modified method of fundamental solution (MMFS), was proposed by Young and his coworkers (Young 2005, Young 2006a, Young 2006b). The solution in MMFS is represented by a distribution of the kernel functions of double layer fundamental solutions. By using the desingularization technique to regularize the singularity and hyper singularity of the kernel functions, the source points can be located on the real boundary as well as the collocation points (figure 3.3) and therefore the diagonal terms of influence matrices are determined. The main difficulty of the coincidence of the source and collocation points then can be avoided.

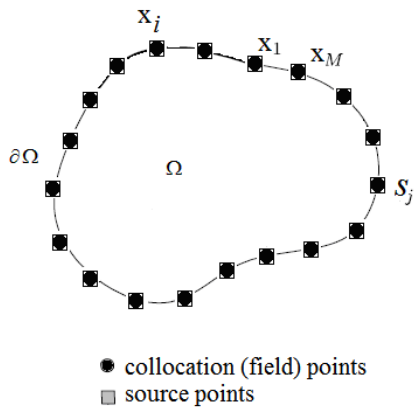

Figure 3.3. Schematic diagram which explains the node distribution in MMFS.

3.2.1 MMFS for solving the Laplace equation

Consider a boundary value problem with a potential $u(\mathrm{x})$, which satisfies the Laplace equation as described by equation (3.1)-(3.3), we denote the BCs here as

$$u(\mathrm{x}) = \overline{u}\,, \quad \mathrm{x} \in \partial\Omega_1\,, \tag{3.13}$$

$$q(\mathrm{x}) = \overline{q}\,, \quad \mathrm{x} \in \partial\Omega_2\,, \tag{3.14}$$

where

$$q(\mathrm{x}) = \frac{\partial u(\mathrm{x})}{\partial \nu(\mathrm{x})}. \tag{3.15}$$

By employing the radial basis functions (RBF) technique (Chen 2002), the representation of the solution for interior problem can be approximated in terms of the coefficients α_j of the source points s_j as

$$u(\mathrm{x}_i) = \sum_{j=1}^{N} A^{(\mathrm{i})}(s_j, \mathrm{x}_i)\alpha_j\,, \tag{3.16}$$

$$q(\mathrm{x}_i) = \sum_{j=1}^{N} B^{(\mathrm{i})}(s_j, \mathrm{x}_i)\alpha_j \,, \tag{3.17}$$

where $A^{(\mathrm{i})}(s_j, \mathrm{x}_i)$ is RBF, in which the superscript (i) denotes the interior domain, α_j is the jth unknown coefficients (strength of the singularities), s_j is jth source point, x_i is ith observation point, N is the number of source points and the chosen RBFs in Young's paper (2005) are the double layer potentials in the potential theory and can be found in (Chen 2002a, Chen 2002b) as

$$A^{(\mathrm{i})}(s_j, \mathrm{x}_i) = \frac{-\left((\mathrm{x}_i - s_j), n_j\right)}{r_{ij}^2} \,, \tag{3.18}$$

$$B^{(\mathrm{i})}(s_j, \mathrm{x}_i) = \frac{\partial A^{(\mathrm{i})}(s_j, \mathrm{x}_i)}{\partial \nu_{\mathrm{x}_i}} = \frac{\left((\mathrm{x}_i - s_j), n_j\right)\left((\mathrm{x}_i - s_j), \overline{n}_i\right)}{r_{ij}^4} - \frac{\left(n_j, \overline{n}_i\right)}{r_{ij}^2}, \tag{3.19}$$

where

$$\overline{r}_{ij} = \left| s_j - \mathrm{x}_i \right|, \tag{3.20}$$

and $(,)$ denotes the inner product of two vectors, n_j is the normal vector at s_j, and $\overline{n}_i$ is the normal vector at x_i. The coefficients α_j $(j = 1, ..., N)$ are determined so that BCs is satisfied at the boundary points x_i $(i = 1, ..., N)$.

By collocating N field points to match with the BCs from equation (3.16) for Dirichlet problems and equation (3.17) for the Neumann problems, we have the following linear systems of the form

$$\begin{bmatrix} a_{1,1} & a_{1,2} & \cdots & a_{1,N} \\ a_{2,1} & a_{2,2} & \cdots & a_{2,N} \\ \vdots & \vdots & \ddots & \vdots \\ a_{N,1} & a_{N,2} & \cdots & a_{N,N} \end{bmatrix} \{\alpha_j\} = \left[A^{(i)} \right] \{\alpha_j\} = \{\overline{u}\}, \tag{3.21}$$

$$\begin{bmatrix} b_{1,1} & b_{1,2} & \cdots & b_{1,N} \\ b_{2,1} & b_{2,2} & \cdots & b_{2,N} \\ \vdots & \vdots & \ddots & \vdots \\ b_{N,1} & b_{N,2} & \cdots & b_{N,N} \end{bmatrix} \{\alpha_j\} = \left[B^{(i)} \right] \{\alpha_j\} = \{\bar{q}\}, \tag{3.22}$$

where

$$a_{i,j} = A^{(i)}(s_j, \mathrm{x}_i), \qquad i, j = 1, 2, \ldots, N, \tag{3.23}$$

$$b_{i,j} = B^{(i)}(s_j, \mathrm{x}_i), \qquad i, j = 1, 2, \ldots, N. \tag{3.24}$$

For the mixed-type problems, a linear combination of equations (3.21) and (3.22) is made to satisfy the mixed-type boundary conditions (BCs). After solving the unknown density coefficients α_j ($j = 1, \ldots, N$) with the linear algebraic solver, the solutions for the interested domain are calculated from the field equations (3.16) and (3.17).

When the collocation point x_i coincide with the source point s_j, equations (3.16) and (3.17) will become singular. Equations (3.16) and (3.17) for the interior problems need to be regularized by using special treatment of subtracting and adding-back technique (Tournour 1999, Hwang 2002) as follows:

$$\begin{aligned} u(\mathrm{x}_i) &= \sum_{j=1}^{N} A^{(i)}(s_j, \mathrm{x}_i)\alpha_j \\ &= \sum_{j=1}^{i-1} A^{(i)}(s_j, \mathrm{x}_i)\alpha_j + \sum_{j=i+1}^{N} A^{(i)}(s_j, \mathrm{x}_i)\alpha_j \\ &\quad + \left[\sum_{m=1}^{N} A^{(i)}(s_m, \mathrm{x}_i) - A^{(i)}(s_i, \mathrm{x}_i) \right] \alpha_j \end{aligned}, \qquad x_i \in \partial\Omega \tag{3.25}$$

$$\begin{aligned} q(\mathrm{x}_i) &= \sum_{j=1}^{N} B^{(i)}(s_j, \mathrm{x}_i)\alpha_j \\ &= \sum_{j=1}^{i-1} B^{(i)}(s_j, \mathrm{x}_i)\alpha_j + \sum_{j=i+1}^{N} B^{(i)}(s_j, \mathrm{x}_i)\alpha_j \\ &\quad - \left[\sum_{m=1}^{N} B^{(i)}(s_m, \mathrm{x}_i) - B^{(i)}(s_i, \mathrm{x}_i) \right] \alpha_j \end{aligned}, \qquad x_i \in \partial\Omega \tag{3.26}$$

$$\{u_i\}=\begin{bmatrix} \sum_{m=1}^{N} a_{1,m}-a_{1,1} & a_{1,2} & \cdots & a_{1,N} \\ a_{2,1} & \sum_{m=1}^{N} a_{2,m}-a_{2,2} & \cdots & a_{2,N} \\ \vdots & \vdots & \ddots & \vdots \\ a_{N,1} & a_{N,2} & \cdots & \sum_{m=1}^{N} a_{N,m}-a_{N,N} \end{bmatrix}\{\alpha_j\}, \tag{3.27}$$

$$\{q_i\}=\begin{bmatrix} -\left(\sum_{m=1}^{N} b_{1,m}-b_{1,1}\right) & b_{1,2} & \cdots & b_{1,N} \\ b_{2,1} & -\left(\sum_{m=1}^{N} b_{2,m}-b_{2,2}\right) & \cdots & b_{2,N} \\ \vdots & \vdots & \ddots & \vdots \\ b_{N,1} & b_{N,2} & \cdots & -\left(\sum_{m=1}^{N} b_{N,m}-b_{N,N}\right) \end{bmatrix}\{\alpha_j\} \tag{3.28}$$

.

In a similar way, the subtracting and adding-back technique was applied to the exterior problems. The diagonal terms of the two influence matrices for both interior and exterior problems can also be derived analytically for a circular domain as shown in (Young 2005).

3.2.2 Regularized meshless method (RMM)

The regularized meshless method (RMM) (Chen 2006), which based on the MMFS, is developed to solve two-dimensional Laplace problem with multiply-connected domain.

Consider a Laplace equation as described by equation (3.1), subject to the BCs as

$$u(\mathrm{x})=\overline{u}\,,\ \text{for}\ \mathrm{x}\in\partial\Omega_t^{\overline{u}}\,,\ \ t=1,2,3,...m\,, \tag{3.29}$$

$$q(\mathrm{x})=\overline{q}\,,\ \text{for}\ \mathrm{x}\in\partial\Omega_t^{\overline{q}}\,,\ \ t=1,2,3,...m\,. \tag{3.30}$$

where $q(\mathrm{x})=\partial u(\mathrm{x})/\partial\nu(\mathrm{x})$, m is the total number of boundaries including $m-1$ numbers of inner boundaries and one outer boundary (the m th boundary), $\partial\Omega_t^{\overline{u}}$ is the

essential boundary (Dirichlet boundary) of the t th boundary in which the potential is prescribed by $\overline{u}$ and $\partial\Omega_t^{\overline{q}}$ is the natural boundary (Neumann boundary) of the t th boundary in which the flux is prescribed by $\overline{q}$. Both $\partial\Omega_t^{\overline{u}}$ and $\partial\Omega_t^{\overline{q}}$ construct the whole boundary of the domain Ω as shown in figure 3.4.

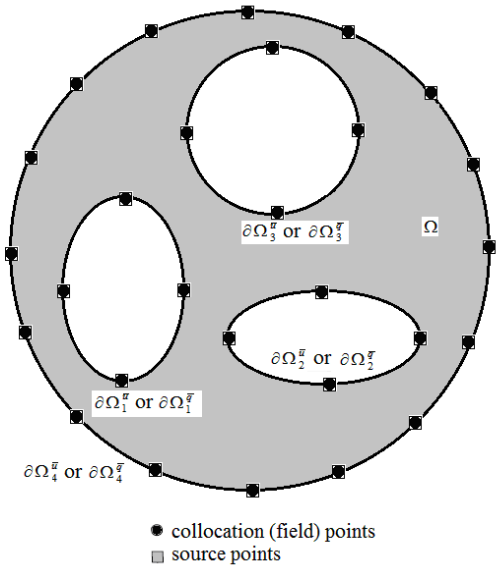

Figure 3.4. Schematic diagram which explains the node distribution in RMM.

By employing the RBF technique (Chen 2002, Cheng 2000), the representation of the solution for multiply-connected problem as shown in figure 3.4 can be expressed in terms of the α_j at s_j as

$$\begin{aligned} u(\mathrm{x}_i) &= \sum_{j=1}^{N} T(s_j, \mathrm{x}_i)\alpha_j \\ &= \sum_{j=1}^{N_1} T(s_j, \mathrm{x}_i)\alpha_j + \sum_{j=N_1+1}^{N_1+N_2} T(s_j, \mathrm{x}_i)\alpha_j \\ &+ \cdots + \sum_{j=N_1+N_2+\cdots+N_{m-1}+1}^{N} T(s_j, \mathrm{x}_i)\alpha_j, \end{aligned} \tag{3.31}$$

$$
\begin{aligned}
q(\mathrm{x}_i) &= \sum_{j=1}^{N} M(s_j, \mathrm{x}_i)\alpha_j \\
&= \sum_{j=1}^{N_1} M(s_j, \mathrm{x}_i)\alpha_j + \sum_{j=N_1+1}^{N_1+N_2} M(s_j, \mathrm{x}_i)\alpha_j \\
&+ \cdots + \sum_{j=N_1+N_2+\cdots+N_{m-1}+1}^{N} M(s_j, \mathrm{x}_i)\alpha_j,
\end{aligned} \tag{3.32}
$$

where α_j is the jth unknown coefficients (strength of the singularities), s_j is jth source point, x_i is ith observation point, N_1, N_2, ..., N_{m-1}, are the numbers of source points on $m-1$ numbers of inner boundaries, respectively, N_m is the number of source points on the outer boundary, while N is the total numbers of source points $N = N_1 + N_2 + \ldots + N_{m-1} + N_m$. The chosen bases are the double-layer potentials (Chen 2002a, Chen 2002b, Young 2005) as

$$
T(s_j, \mathrm{x}_i) = \frac{-\left((\mathrm{x}_i - s_j), n_j\right)}{r_{ij}^2}\ , \tag{3.33}
$$

$$
M(s_j, \mathrm{x}_i) = \frac{\partial T(s_j, \mathrm{x}_i)}{\partial \nu(\mathrm{x}_i)} = \frac{\left((\mathrm{x}_i - s_j), n_j\right)\left((\mathrm{x}_i - s_j), \bar{n}_i\right)}{r_{ij}^4} - \frac{\left(n_j, \bar{n}_i\right)}{r_{ij}^2}, \tag{3.34}
$$

where $(,)$ denotes the inner product of two vectors, $r_{ij} = \left| s_j - \mathrm{x}_i \right|$, n_j is the normal vector at s_j, and $\bar{n}_i$ is the normal vector at x_i .

As the field point x_i coincide with the source point s_j, equations. (3.33) and (3.34) will become singular. Equations (3.33) and (3.34) for the multiply-connected problems need to be regularized by using the regularization of subtracting and adding back technique which same as MMFS (Young 2005):

$$
\begin{aligned}
u(\mathrm{x}_i^I) &= \sum_{j=1}^{N_1} T(s_j^I, \mathrm{x}_i^I)\alpha_j + \cdots + \sum_{j=N_1+\cdots+N_{t-1}+1}^{N_1+\cdots+N_t} T(s_j^I, \mathrm{x}_i^I)\alpha_j \\
&+ \cdots + \sum_{j=N_1+\cdots+N_{m-2}+1}^{N_1+\cdots+N_{m-1}} T(s_j^I, \mathrm{x}_i^I)\alpha_j + \sum_{j=N_1+\cdots+N_{m-1}+1}^{N} T(s_j^O, \mathrm{x}_i^I)\alpha_j \\
&- \sum_{j=N_1+\cdots+N_{t-1}+1}^{N_1+\cdots+N_t} T(s_j^I, \mathrm{x}_i^I)\alpha_i
\end{aligned} \tag{3.35}
$$

for $\mathrm{x}_i^I \in \partial\Omega_t$, $t=1,2,3,\ldots,m-1$, where x_i^I is located on the inner boundary $(t=1,\ 2,\ ...,\ m-1)$ and the superscript I and O denote the inward and outward normal vectors, respectively, and

$$\sum_{j=N_1+\cdots+N_{t-1}+1}^{N_1+\cdots+N_t} T(s_j^I,\mathrm{x}_i^I)=0,\quad \mathrm{x}_i^I \in \partial\Omega_t,\quad t=1,2,3,\ldots,m-1. \tag{3.36}$$

Therefore, we can obtain:

$$\begin{aligned} u(\mathrm{x}_i^I) &= \sum_{j=1}^{N_1} T(s_j^I,\mathrm{x}_i^I)\alpha_j+\cdots+\sum_{j=N_1+\cdots+N_{t-1}+1}^{i-1} T(s_j^I,\mathrm{x}_i^I)\alpha_j \\ &+\sum_{j=i+1}^{N_1+\cdots+N_t} T(s_j^I,\mathrm{x}_i^I)\alpha_j+\cdots+\sum_{j=N_1+\cdots+N_{m-2}+1}^{N_1+\cdots+N_{m-1}} T(s_j^I,\mathrm{x}_i^I)\alpha_j \\ &+\sum_{j=N_1+\cdots+N_{m-1}+1}^{N} T(s_j^O,\mathrm{x}_i^I)\alpha_j-\left[\sum_{j=N_1+\cdots+N_{t-1}+1}^{N_1+\cdots+N_t} T(s_j^I,\mathrm{x}_i^I)-T(s_i^I,\mathrm{x}_i^I)\right]\alpha_i, \end{aligned} \tag{3.37}$$

for $\mathrm{x}_i^I \in \partial\Omega_t$, $t=1,2,3,\ldots,m-1$.

When the field point locates on the outer boundary ($p=m$), equation (3.35) becomes

$$\begin{aligned} u(\mathrm{x}_i^O) &= \sum_{j=1}^{N_1} T(s_j^I,\mathrm{x}_i^O)\alpha_j+\sum_{j=N_1+1}^{N_1+N_2} T(s_j^I,\mathrm{x}_i^O)\alpha_j+\cdots \\ &+\sum_{j=N_1+\cdots+N_{m-2}+1}^{N_1+\cdots+N_{m-1}} T(s_j^I,\mathrm{x}_i^O)\alpha_j+\sum_{j=N_1+\cdots+N_{m-1}+1}^{N} T(s_j^O,\mathrm{x}_i^O)\alpha_j, \\ &-\sum_{j=N_1+\cdots+N_{m-1}+1}^{N} T(s_j^I,\mathrm{x}_i^I)\alpha_i \end{aligned} \tag{3.38}$$

for $\mathrm{x}_i^{O\ and\ I} \in \partial\Omega_t$, $t=m$, where

$$\sum_{j=N_1+\cdots+N_{m-1}+1}^{N} T(s_j^I,\mathrm{x}_i^I)\alpha_i=0,\quad \mathrm{x}_i^I \in \partial\Omega_t,\quad t=m. \tag{3.39}$$

Hence, we obtain

$$
\begin{aligned}
u(\mathrm{x}_i^O) = & \sum_{j=1}^{N_1} T(s_j^I, \mathrm{x}_i^O)\alpha_j + \sum_{j=N_1+1}^{N_1+N_2} T(s_j^I, \mathrm{x}_i^O)\alpha_j + \cdots \\
& + \sum_{j=N_1+\cdots+N_{m-2}+1}^{N_1+\cdots+N_{m-1}} T(s_j^I, \mathrm{x}_i^O)\alpha_j + \sum_{j=N_1+\cdots+N_{m-1}+1}^{i-1} T(s_j^O, \mathrm{x}_i^O)\alpha_j \\
& + \sum_{j=i+1}^{N} T(s_j^O, \mathrm{x}_i^O)\alpha_j - \left[\sum_{j=N_1+\cdots+N_{m-1}+1}^{N} T(s_j^I, \mathrm{x}_i^I) - T(s_i^O, \mathrm{x}_i^O) \right] \alpha_i
\end{aligned}
\quad , \tag{3.40}
$$

for $\mathrm{x}_i^{I \text{ and } O} \in \partial\Omega_t$, $t = m$.

Similarly, the Neumann boundary equations can be obtained as

$$
\begin{aligned}
q(\mathrm{x}_i^I) = & \sum_{j=1}^{N_1} M(s_j^I, \mathrm{x}_i^I)\alpha_j + \cdots + \sum_{j=N_1+\cdots+N_{t-1}+1}^{N_1+\cdots+N_t} M(s_j^I, \mathrm{x}_i^I)\alpha_j + \cdots \\
& + \sum_{j=N_1+\cdots+N_{m-2}+1}^{N_1+\cdots+N_{m-1}} M(s_j^I, \mathrm{x}_i^I)\alpha_j + \sum_{j=N_1+\cdots+N_{m-1}+1}^{N} M(s_j^O, \mathrm{x}_i^I)\alpha_j \\
& + \sum_{j=N_1+\cdots+N_{t-1}+1}^{N_1+\cdots+N_t} M(s_j^I, \mathrm{x}_i^I)\alpha_i
\end{aligned}
\quad , \tag{3.41}
$$

for $\mathrm{x}_i^I \in \partial\Omega_t$, $t = 1,2,3,\ldots,m-1$.

Where

$$
\sum_{j=N_1+\cdots+N_{t-1}+1}^{N_1+\cdots+N_t} M(s_j^I, \mathrm{x}_i^I) = 0
\quad , \tag{3.42}
$$

for $\mathrm{x}_i^I \in \partial\Omega_t$, $t = 1,2,3,\ldots,m-1$. Thus, we have

$$
\begin{aligned}
q(\mathrm{x}_i^I) = & \sum_{j=1}^{N_1} M(s_j^I, \mathrm{x}_i^I)\alpha_j + \cdots + \sum_{j=N_1+\cdots+N_{t-1}+1}^{i-1} M(s_j^I, \mathrm{x}_i^I)\alpha_j \\
& + \sum_{j=i+1}^{N_1+\cdots+N_t} M(s_j^I, \mathrm{x}_i^I)\alpha_j + \cdots + \sum_{j=N_1+\cdots+N_{m-1}+1}^{N_1+\cdots+N_{m-1}} M(s_j^I, \mathrm{x}_i^I)\alpha_j \\
& + \sum_{j=N_1+\cdots+N_{m-1}+1}^{N} M(s_j^O, \mathrm{x}_i^I)\alpha_j - \left[\sum_{j=N_1+\cdots+N_{t-1}+1}^{N_1+\cdots+N_t} M(s_j^I, \mathrm{x}_i^I) - M(s_i^I, \mathrm{x}_i^I) \right] \alpha_i
\end{aligned}
\quad , \tag{3.43}
$$

for $\mathrm{x}_i^I \in \partial\Omega_t,\ \ t=1,2,3,\ldots,m-1.$

When the field point locates on the outer boundary ($p=m$), equation (3.41) yields

$$\begin{aligned} q(\mathrm{x}_i^O) = & \sum_{j=1}^{N_1} M(s_j^I, \mathrm{x}_i^O)\alpha_j + \sum_{j=N_1+1}^{N_1+N_2} M(s_j^I, \mathrm{x}_i^O)\alpha_j + \cdots \\ & + \sum_{j=N_1+\cdots+N_{m-2}+1}^{N_1+\cdots+N_{m-1}} M(s_j^I, \mathrm{x}_i^O)\alpha_j + \sum_{j=N_1+\cdots+N_{m-1}+1}^{N} M(s_j^O, \mathrm{x}_i^O)\alpha_j \\ & - \sum_{j=N_1+\cdots+N_{m-1}+1}^{N} M(s_j^I, \mathrm{x}_i^I)\alpha_i \end{aligned}, \tag{3.44}$$

Where

$$\sum_{j=N_1+\cdots+N_{m-1}+1}^{N} M(s_j^I, \mathrm{x}_i^I) = 0, \tag{3.45}$$

for $\mathrm{x}_i^I \in \partial\Omega_t,\ \ t=m$. Thus, we have

$$\begin{aligned} q(\mathrm{x}_i^O) = & \sum_{j=1}^{N_1} M(s_j^I, \mathrm{x}_i^O)\alpha_j + \sum_{j=N_1+1}^{N_1+N_2} M(s_j^I, \mathrm{x}_i^O)\alpha_j + \cdots \\ & + \sum_{j=N_1+\cdots+N_{m-2}+1}^{N_1+\cdots+N_{m-1}} M(s_j^I, \mathrm{x}_i^O)\alpha_j + \sum_{j=N_1+\cdots+N_{m-1}+1}^{i-1} M(s_j^O, \mathrm{x}_i^O)\alpha_j \\ & + \sum_{j=i+1}^{N} M(s_j^O, \mathrm{x}_i^O)\alpha_j - \left[\sum_{j=N_1+\cdots+N_{m-1}+1}^{N} M(s_j^I, \mathrm{x}_i^I) - M(s_i^O, \mathrm{x}_i^O) \right] \alpha_i \end{aligned}, \tag{3.46}$$

for $\mathrm{x}_i^{O \text{ and } I} \in \partial\Omega_t,\ \ t=m.$

The detailed derivation of equations (3.36) and (3.39) are given in (Young 2005), According to the dependence of the normal vectors for inner and outer boundaries, their relationships are

$$\begin{cases} T\left(s_j^I,\ \mathrm{x}_i^I\right) = -T\left(s_j^O,\ \mathrm{x}_i^O\right), & i \neq j, \\ T\left(s_j^I,\ \mathrm{x}_i^I\right) = T\left(s_j^O,\ \mathrm{x}_i^O\right), & i = j, \end{cases} \tag{3.47}$$

$$M\left(s_j^I,\ \mathrm{x}_i^I\right) = M\left(s_j^O,\ \mathrm{x}_i^O\right), \tag{3.48}$$

where the left and right sides of the equal sign in equations (3.43) and (3.44) denote the kernels for field point and source point with the unit inward and outward normal vectors, respectively.

3.3 Boundary distributed source (BDS) method

The boundary distributed source (BDS) method (Liu 2010), is based on the same concept in MFS. In the BDS method the source points and filds points coincide and both are placed on the boundary of the problem domain directly, unlike the traditional MFS that requires a fictitious boundary for placing the source points. To remove the singularities of the fundamental solutions, the concentrated point sources can be replaced by distributed sources over areas (for 2D problems) or volumes (for 3D problems) covering the source points. For Dirichlet boundary conditions, all the coefficients (either diagonal or off-diagonal) in the systems of equations can be determined analytically, however, the diagonal coefficients for Neumann boundary conditions is determined indirectly.

Consider the Laplace equation in a 2D domain Ω governed by equation (3.1), under the BCs of (3.13) and (3.14). N distributed sources were placed at point s_j (j=1, 2, ..., N) on boundary $\partial\Omega$, as shown in figure 3.5. Then u can be given by the following expression satisfies the governing equation (3.1):

$$u(\mathrm{x}) = \sum_{j=1}^{N} \int_{A(s_j)} G(\mathrm{x}, s_j')\, dA(s_j')\, \mu_j \quad \text{for } x \in \partial\Omega_1, \tag{3.49}$$

where $A(s_j)$ can be a line segment or an area covering point s_j on the boundary, and

$$G(\mathrm{x}, s_j') = -\frac{1}{2\pi}\ln(r) \ , \tag{3.50}$$

is the fundamental solution for 2D Laplace equation, and r is the distance between the field point x and source point s_j', and μ_j an unknown intensity of the distributed source at s_j.

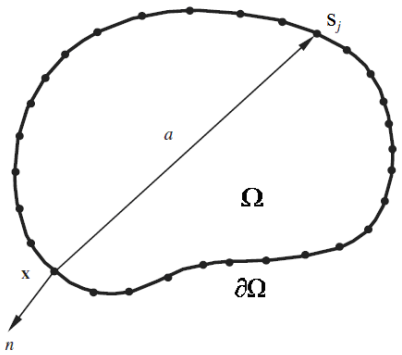

Figure 3.5. A domain Ω with boundary ∂Ω, the collocation point x, and center s_j of a source.

In BDS, we consider the case that A(s) is a circular disk of radius R_s and centered at point s_j on the boundary ∂Ω (see figure 3.6) for 2D problems. The integration of the fundamental solution $G(\mathrm{x}, s)$ on a circular disk A(s) yields the following analytic results:

$$\tilde{G}(\mathrm{x}, s) = \int_{A(s)} G(\mathrm{x}, s')dA(s') = \begin{cases} \dfrac{R_s^2}{2}\ln(\dfrac{1}{a}) & \text{for } a \geq R_s \\ \dfrac{R_s^2}{2}\ln(\dfrac{1}{R_s}) - \dfrac{R_s^2 - a^2}{4} & \text{for } a \leq R_s \end{cases}, \tag{3.51}$$

in which a is the distance between x and s (center of the disk).

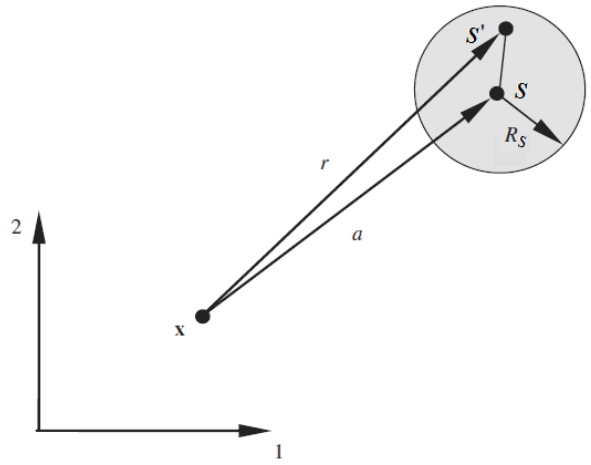

Figure 3.6. A Distributed source on a circular disk centered at point s and with radius R_s.

By substituting equation (3.51), we can rewrite equation (3.50) as follows

$$u(\mathrm{x}) = \sum_{j=1}^{N} \tilde{G}(\mathrm{x}, s_j)\mu_j \quad \text{for} \quad \mathrm{x} \in \partial\Omega_1, \tag{3.52}$$

The boundary conditions in equations (3.13) and (3.14) can be satisfied at the field points x_i by adjusting μ_j at the source points s_j, that is, imposing the following conditions:

$$\sum_{j=1}^{N} \tilde{G}_{ij}\mu_j = \bar{u}_i \quad \text{for} \quad \mathrm{x} \in \partial\Omega_1, \tag{3.53}$$

$$\sum_{j=1}^{N} \tilde{K}_{ij}\mu_j = \bar{q}_i \quad \text{for} \quad \mathrm{x} \in \partial\Omega_2, \tag{3.54}$$

where

$$\tilde{G}_{ij} = \tilde{G}(\mathrm{x}_i, s_j), \tag{3.55}$$

and

$$\tilde{K}_{ij} = \tilde{K}(\mathrm{x}_i, s_j)\,, \tag{3.56}$$

with

$$\begin{aligned}\tilde{K}(\mathrm{x}, s) &= \frac{\partial \tilde{G}(\mathrm{x}, s)}{\partial \nu(\mathrm{x})} = \int_{A(\mathrm{y})} K(\mathrm{x}, s')\, dA(s') \\ &= \int_{A(\mathrm{y})} \frac{\partial G(\mathrm{x}, s')}{\partial \nu(\mathrm{x})}\, dA(\mathrm{y}') = \frac{\partial \tilde{G}(\mathrm{x}, s')}{\partial \nu(\mathrm{x})}\,. \\ &= -\frac{R_s^{\,2}}{2a}\frac{\partial a}{\partial \nu(\mathrm{x})}, \quad \text{for } a > R_s\end{aligned} \tag{3.57}$$

Since the valid expressions for $\tilde{K}(\mathrm{x},s)$ when $0 \le a \le R$ are still under investigation, the diagonal term in equation (3.54) needs to be determined indirectly for field points on $\partial\Omega_2$. In BDS, the method proposed by Sarler (2009) is applied to determine the diagonal coefficient in equation (3.54). In this approach, the author first assumes a constant solution, *e.g.*, $u = c$ everywhere. Then, from equation (3.53) the corresponding densities μ_j^c can be solved for all the boundary points. Finally, from equation (3.54) the following expression for the diagonal term using the known density values μ_j^c can be given:

$$\tilde{K}_{ii} = \frac{1}{\mu_i^c} \sum_{\substack{j=1 \\ j \neq 1}}^{N} \tilde{K}_{ij} \mu_j^c\,. \tag{3.58}$$

Finally, the following standard linear system of equations is formed after applying equations (3.53) or (3.54) at all the field points:

$$\begin{bmatrix} a_{11} & a_{12} & \cdots & a_{1N} \\ a_{21} & a_{22} & \cdots & a_{2N} \\ \vdots & \vdots & \ddots & \vdots \\ a_{N1} & a_{N2} & \cdots & a_{NN} \end{bmatrix} \begin{Bmatrix} \mu_1 \\ \mu_2 \\ \vdots \\ \mu_N \end{Bmatrix} = \begin{Bmatrix} b_1 \\ b_2 \\ \vdots \\ b_N \end{Bmatrix}, \tag{3.59}$$

or

$$\mathbf{A}\boldsymbol{\mu} = \mathbf{b}, \tag{3.60}$$

where $\mathbf{A}$ is the coefficient matrix, $\boldsymbol{\mu}$ the unknown density vector, and $\mathbf{b}$ the right-hand side vector. Once all the values of μ_j are determined by solving this equation, the potential at any point inside the domain or on the boundary can be evaluated using equation(3.52).

3.4 Singular boundary method (SBM)

Like the MFS, the singular boundary method (SBM) (Chen 2009a, Chen 2009b Chen 2010, Gu 2011) employs the singular fundamental solution of the governing equation of interest as the interpolation basis function. However, the source and field points of the SBM coincide on the physical boundary without the requirement of introducing fictitious boundary. In order to avoid the singularity, this method proposes an inverse interpolation technique (IIT) to evaluate the singular diagonal elements of the MFS coefficient matrix.

In SBM, the MFS solution $u(\mathrm{x})$ and $\dfrac{\partial u(\mathrm{x})}{\partial \nu(\mathrm{x})}$ of the Laplace problem can be expressed by a linear combination of fundamental solutions with respect to different source points s_j as follows:

$$u(\mathrm{x}_i) = \sum_{j=1}^{N} \alpha_j u^*(\mathrm{x}_i, s_j), \tag{3.61}$$

$$q(\mathrm{x}_i) = \frac{\partial u(\mathrm{x}_i)}{\partial \nu(\mathrm{x}_i)} = \sum_{j=1}^{N} \alpha_j \frac{\partial u^*(\mathrm{x}_i, s_j)}{\partial \nu(\mathrm{x}_i)}, \tag{3.62}$$

where x_i is the i th field point, s_j the j th source point, α_j the j th unknown intensity of the distributed source at s_j, N the numbers of source points and

$$u^*(\mathrm{x}_i, s_j) = -\frac{1}{2\pi} \ln \left| \mathrm{x}_i - s_j \right|, \text{ for } \mathrm{x} \in \partial\Omega_2, \tag{3.63}$$

is the fundamental solution of two-dimensional Laplace equation.

The SBM interpolation formula is given by (Chen 2010)

$$u(\mathrm{x}_i) = \sum_{j=1, i \neq j}^{N} \alpha_j u^*(\mathrm{x}_i, s_j) + \alpha_i u_{ii}, \tag{3.64}$$

$$q(\mathrm{x}_i) = \frac{\partial u(\mathrm{x}_i)}{\partial \nu(\mathrm{x}_i)} = \sum_{j=1, i \neq j}^{N} \alpha_j \frac{\partial u^*(\mathrm{x}_i, s_j)}{\partial \nu(\mathrm{x}_i)} + \alpha_i q_{ii}, \tag{3.65}$$

where u_{ii} and q_{ii} are the diagonal elements of the SBM interpolation matrix.

When the field point x_i coincide with the source point s_j, the distance between these two boundary nodes trends to zero. This would cause boundary equations (3.64) and (3.65) present singularities. By using the subtracting and adding-back technique, the regularized expressions for the Neumann boundary equation (3.65) can be written as:

$$q(\mathrm{x}_i) = \sum_{j=1}^{N} (\alpha_j - \alpha_i) \frac{\partial u^*(\mathrm{x}_i, s_j)}{\partial \nu(\mathrm{x}_i)} + \alpha_i \sum_{j=1}^{N} \frac{\partial u^*(\mathrm{x}_i, s_j)}{\partial \nu(\mathrm{x}_i)}, \tag{3.66}$$

Note that, when i is equal to j,

$$(\alpha_j - \alpha_i) \frac{\partial u^*(\mathrm{x}_i, s_j)}{\partial \nu(\mathrm{x}_i)} = 0, \tag{3.67}$$

so there is no singularity in the first right side term. To remove the singularity of the second right side term, we rewrite equation (3.66) as follows:

$$q(\mathrm{x}_i) = \sum_{j=1, i\neq j}^{N} (\alpha_j - \alpha_i) \frac{\partial u^*(\mathrm{x}_i, s_j)}{\partial \nu(\mathrm{x}_i)} + \alpha_i \sum_{j=1}^{N} \left(\frac{\partial u^*(\mathrm{x}_i, s_j)}{\partial \nu(\mathrm{x}_i)} + \frac{\partial u^{*c}(\mathrm{x}_i, s_j)}{\partial \nu(s_j)} \right), \tag{3.68}$$

in which

$$\sum_{j=1}^{N} \frac{\partial u^{*c}(\mathrm{x}_i, s_j)}{\partial \nu(s_j)} = 0, \tag{3.69}$$

and $u^{*c}(\mathrm{x}_i, s_j)$ denotes the fundamental solution of the exterior problems. The detail derivations of equation (3.69) are given in (Chen 2012).

According to the dependency of the outward normal vectors on the two kernel functions of interior and exterior problems, we can obtain the following relationships (Young 2005):

$$\begin{cases} \dfrac{\partial u^*(\mathrm{x}_i, s_j)}{\partial \nu(s_j)} = -\dfrac{\partial u^{*c}(\mathrm{x}_i, s_j)}{\partial \nu(s_j)}, & i \neq j \\ \dfrac{\partial u^*(\mathrm{x}_i, s_j)}{\partial \nu(s_j)} = \dfrac{\partial u^{*c}(\mathrm{x}_i, s_j)}{\partial \nu(s_j)}, & i = j \end{cases}, \tag{3.70}$$

$$\begin{aligned} &\frac{\partial u^*(\mathrm{x}_i, s_j)}{\partial \nu(\mathrm{x}_i)} + \frac{\partial u^*(\mathrm{x}_i, s_j)}{\partial \nu(s_j)} \\ &= \frac{\partial u^*(\mathrm{x}_i, s_j)}{\partial \mathrm{x}^{(1)}} (n_1(\mathrm{x}_i) - n_1(s_j)) + \frac{\partial u^*(\mathrm{x}_i, s_j)}{\partial \mathrm{x}^{(2)}} (n_2(\mathrm{x}_i) - n_2(s_j)) \end{aligned}, \tag{3.71}$$

where the indicial notation for the coordinates of points x_i, i.e., $(\mathrm{x}^{(1)}, \mathrm{x}^{(2)})$ is employed. For arbitrarily smooth boundary, we assume that the source point s_j moves gradually close to the field point x_i along a line segment, thus we have

$$\lim_{s_j \to x_i} \frac{\partial u^*(\mathrm{x}_i, s_j)}{\partial \nu(\mathrm{x}_i)} + \frac{\partial u^*(\mathrm{x}_i, s_j)}{\partial \nu(s_j)} = 0, \tag{3.72}$$

From equations (3.70) and (3.72), equation (3.68) can be rewritten as

$$\begin{aligned} q(\mathrm{x}_i) &= \sum_{j=1, i\neq j}^{N} (\alpha_j - \alpha_i) \frac{\partial u^*(\mathrm{x}_i, s_j)}{\partial \nu(\mathrm{x}_i)} + \alpha_i \sum_{j=1, i\neq j}^{N} \left(\frac{\partial u^*(\mathrm{x}_i, s_j)}{\partial \nu(\mathrm{x}_i)} - \frac{\partial u^*(\mathrm{x}_i, s_j)}{\partial \nu(s_j)} \right) \\ &= \sum_{j=1, i\neq j}^{N} \alpha_j \frac{\partial u^*(\mathrm{x}_i, s_j)}{\partial \nu(\mathrm{x}_i)} - \alpha_i \sum_{j=1, i\neq j}^{N} \frac{\partial u^*(\mathrm{x}_i, s_j)}{\partial \nu(s_j)} \end{aligned}. \tag{3.73}$$

It can be seen from the above equation (3.73) that the original singular term $\frac{\partial u^{*c}(\mathrm{x}_i, s_j)}{\partial \nu(s_j)}$ in equation (3.68) under $i = j$ has been transformed into the following regular terms

$$q_{ii} = -\sum_{j=1, i\neq j}^{N} \frac{\partial u^*(\mathrm{x}_i, s_j)}{\partial \nu(s_j)}, \tag{3.74}$$

The regularized expressions for the Dirichlet boundary equation (3.64) can be calculated by using the strategy proposed by Sarler (2009), in which the singular value of $u(\mathrm{x})$ is considered as an average of the fundamental solution over a portion of the boundary. However, the integral calculation makes this strategy more complex and less efficient. In SBM, the regularized expressions of the Dirichlet boundary equation can be calculated in a new indirect way, namely an improved inverse interpolation technique (IIT), which is different from the original IIT in that it does not require the sampling nodes.

First, we assuming a pure Neumann problem with all the boundary values set as

$$\overline{q}(\mathrm{x}) = \frac{\partial \overline{u}(\mathrm{x})}{\partial \nu(\mathrm{x})}, \tag{3.75}$$

where $\bar{u}(x)$ (named as sample solution in SBM) is an arbitrary known particular solution of Laplace equation, such as

$$\bar{u}(\mathrm{x}) = \mathrm{x}^{(1)} - \mathrm{x}^{(2)}. \tag{3.76}$$

Then, from the regularized Neumann boundary equation (3.73), we obtain:

$$\bar{q}\ (\mathrm{x}_i) = \sum_{j=1, i\neq j}^{N} \alpha'_j \frac{\partial u^*(\mathrm{x}_i, s_j)}{\partial \nu(\mathrm{x}_i)} - \alpha'_i \sum_{j=1, i\neq j}^{N} \frac{\partial u^*(\mathrm{x}_i, s_j)}{\partial \nu(s_j)}, \quad i = 1,\ 2,\ ...,\ N, \tag{3.77}$$

where α'_j are unknown coefficients and can be calculated directly by solving the above equation (3.77).

Finally, substituting the calculated α'_j into the Dirichlet boundary equation (3.64) we can get the following algebraic equations:

$$\bar{u}(\mathrm{x}_i) = \sum_{j=1, i\neq j}^{N} \alpha'_j u^*(\mathrm{x}_i, s_j) + \alpha'_i u_{ii} + c, \quad i = 1,\ 2,\ ...,\ N, \tag{3.78}$$

where c is a constant and can be solved by using an arbitrary field point inside the domain. For example, suppose $\mathrm{x}_0 = (\mathrm{x}_0^{(1)}, \mathrm{x}_0^{(2)})$ is an arbitrary point inside the domain of interest, then the constant c can be calculated by

$$\begin{aligned} c &= \bar{u}(\mathrm{x}_0) - \sum_{j=1}^{N} \alpha'_j u^*(\mathrm{x}_0, s_j) \\ &= (\mathrm{x}_0^{(1)} + \mathrm{x}_0^{(2)}) - \sum_{j=1}^{N} \alpha'_j u^*(\mathrm{x}_0, s_j) \end{aligned}. \tag{3.79}$$

Since the interior field point $x_0 = (x_0^{(1)}, x_0^{(2)})$ is chosen in side the domain and will never coincide with the boundary source point s_j, the function $u^*(x_0, s_j)$ can be calculated directly.

Thus, diagonal terms of $\tilde{G}(p\ , p_j)$ for Dirichlet boundary equation can be calculated as:

$$u_{ii} = \frac{1}{\alpha_i'}\left[\bar{u}(x_i) - c - \sum_{j=1, i\neq j}^{N} \alpha_j' u^*(x_i, s_j)\right],\ \ i = 1,\ 2,\ ...,\ N\ . \tag{3.80}$$

Using the procedure described above, the origin intensity factors for both Neumann and Dirichlet boundary equations (3.64) and (3.65) can be calculated. And the resulting system equations can be formed.

4. Improved boundary distributed source method for EIT forward problem

In the BDS method, all elements of the system matrix can be derived analytically for the Dirichlet boundary conditions without singularity. For the Neumann boundary conditions, however, while off-diagonal elements can be determined analytically the diagonal elements should be obtained indirectly from the constant potential field (Saler 2009). Hence, the indirect determination involves the solution of the system equation. Recently, Kim (2013) suggested an improved BDS (IBDS) method for the Laplace equations to determine the diagonal element for the Neumann boundary conditions by using the fact that the integration of the normal derivative of the potential function over the domain boundary should vanish. In doing so, the IBDS method can remove the procedure to determine indirectly the diagonal elements for the Neumann boundary conditions.

In this section, the IBDS formulation for the EIT forward problem is presented, also a hybrid MM of IBDS and SBM is proposed, in which the regularized expressions of the Dirichlet boundary equation is carried out in a new indirect way, namely an improved inverse interpolation technique used in SBM by Chen *et al.*(2012).

4.1 IBDS for EIT forward problem

4.1.1 Improved boundary distributed source method (IBDS)

In the BDS formulation (Liu 2010), a number of source points p_j ($j = 1, 2, \cdots, N$) are selected along the domain boundary. The solution $u(p)$ at a certain field point p is expressed as a linear combination of the fundamental solution integrated over a circle $A(p_j)$ with radius of R_j and centered at the selected source point p_j:

$$u(p)=\sum_{j=1}^{N}\int_{A(p_j)} G(p,s)dA(s)\mu_j=\sum_{j=1}^{N}\tilde{G}(p,p_j)\mu_j \text{ , for } p\in\bar{\Omega}\text{, and } p_j\in\partial\Omega \tag{4.1}$$

where μ_j are the unknown source densities to be determined, $\bar{\Omega}$ is the closure of the domain Ω, and G is the fundamental solution of Laplace equation. The fundamental solution in 2D for the Laplace equation is of the form:

$$G(p,p_j)=\frac{1}{4\pi}\ln\left|p-p_j\right|^2, \quad \text{for } p,p_j\in\Re^2. \tag{4.2}$$

R_j is the radius of the distributed source. Although, the determination of R_j is not conclusive at present, it is reported that $R_j=l_j/4$ allows quite accurate and stable numerical results in most cases (Liu 2009, Kim 2013). The integration of the fundamental solution can be obtained in a simple form:

$$\tilde{G}(p,p_j)=\begin{cases}\dfrac{R_j^2}{2}\ln\left|p_j-p\right| & \text{for } \left|p_j-p\right|\geq R_j \\ \dfrac{R_j^2}{2}\ln R_j-\dfrac{R_j^2-\left|p_j-p\right|^2}{4} & \text{for } \left|p_j-p\right|\leq R_j\end{cases}. \tag{4.3}$$

In order to impose the Neumann boundary conditions to evaluate the normal flux at the boundary of interest, we should have the expression for the normal derivative of the solution:

$$\begin{aligned} q(p)&=\frac{\partial u(p)}{\partial \nu(p)}=\sum_{j=1}^{N}\int_{A(p_j)}\frac{\partial G(p,p_s)}{\partial \nu(p)}dA(p_s)\mu_j \\ &=\sum_{j=1}^{N}\int_{A(p_j)} Q(p,p_s)dA(p_s)\mu_j \qquad \text{, for } p\in\bar{\Omega} \text{ and } p_j\in\partial\Omega. \\ &=\sum_{j=1}^{N}\tilde{Q}(p,p_j)\mu_j \end{aligned} \tag{4.4}$$

where

$$Q(p,p_s)=\frac{\partial}{\partial \nu}G(p,p_s)$$
$$=-\frac{1}{2\pi}\frac{(p_s-p)\cdot\nu(p)}{|p_s-p|^2}=-\frac{1}{2\pi}\frac{(p_s-p)\cdot\nu(p)}{r^2} \quad . \tag{4.5}$$

The terms $\tilde{Q}(p,p_j)$ for $|p_j-p|\geq R_j$, which correspond to off-diagonal elements, can be easily obtained as

$$\tilde{Q}(p,p_j)=-\frac{R_j^2(p_j-p)\cdot\nu(p)}{2|p_j-p|^2}, \quad \text{for } |p_j-p|\geq R_j. \tag{4.6}$$

Note that

$$\tilde{G}(p,p_j)=\frac{R_j^2}{2}\ln|p_j-p|=\pi R_j^2 G(p,p_j) \quad \text{for} \quad |p_j-p|\geq R_j, \tag{4.7}$$

$$\tilde{Q}(p,p_j)=-\frac{R_j^2(p_j-p)\cdot\nu(p)}{2|p_j-p|^2}=\pi R_j^2 Q(p,p_j) \quad \text{for} \quad |p_j-p|\geq R_j, \tag{4.8}$$

However, $\tilde{Q}(p,p_j)$ for $|p_j-p|<R_j$, which correspond to diagonal elements, is not available and Liu (2010) recommended to determine the terms indirectly from the constant potential field as proposed by Šarler (2009). The IBDS method (Kim 2013) suggests a simple way to determine $\tilde{Q}(p_j,p_j)$ without any matrix inversion. Considering the fact that the boundary integration of the normal gradient of the potential function should vanish, we have

$$\int_{\partial\Omega} q(p)dS(p)=\sum_{j=1}^{N}\int_{\partial\Omega}\tilde{Q}(p,p_j)dS(p)\mu_j=0\,. \tag{4.9}$$

Since equation (4.9) should be satisfied for arbitrary boundary conditions or source density distributions, therefore we have

$$\int_{\partial\Omega} \tilde{Q}(p, p_j) dS(p) = 0, \tag{4.10}$$

and $\tilde{Q}(p_j, p_j)$ can be evaluated as

$$\tilde{Q}(p_j, p_j) \cong -\frac{1}{l_j} \sum_{i=1, i\neq j}^{N} \tilde{Q}(p_i, p_j) l_i, \tag{4.11}$$

where l_i is the length of the ith line segment of the boundary.

4.1.2 IBDS Formulation for EIT with CEM

Considering that the electrodes are spaced equally around the circumference of the outer domain with region boundaries with constant conductivities and has the same size of $|e|$. Each electrode and each gap regions are uniformly placed with m_E and m_G source points, respectively. Hence, the numbers of the electrode and the gap nodes are $M_E = Lm_E$ and $M_G = Lm_G$, respectively. If the number of the source points of the inclusion boundaries is M_D, the total number of nodes is $M = M_E + M_G + M_D$. Here, the subscripts E, G, and D represent the electrode, gap, the anomaly boundary, respectively. The node distributions of a circular domain Ω with an anomaly D located at the center is shown in figure 4.1.

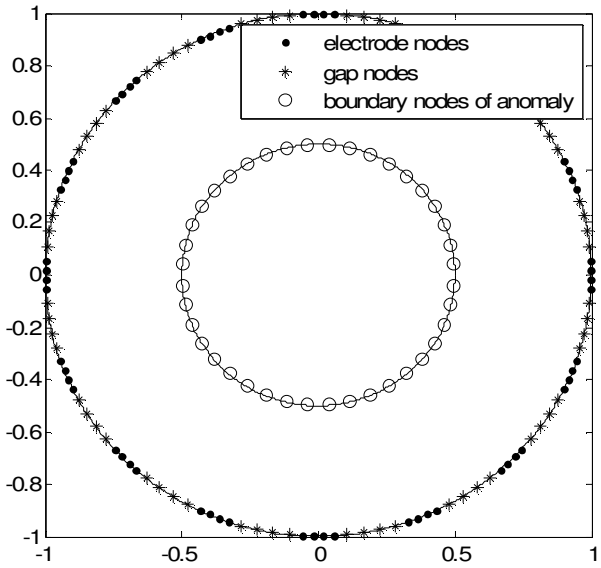

Figure 4.1. Node distributions of a circular domain with an anomaly located at the center.

According to the IBDS formulation, the potential distribution and its normal derivative on the background $\Omega \setminus \bar{D}$ and on the inclusion D can be expressed as

$$u_b(p) = \sum_{j=1}^{M} \tilde{G}(p, p_j)\mu_j^b \quad \text{and} \quad q_b(p) = \sum_{j=1}^{M} \tilde{Q}(p, p_j)\mu_j^b \,, \tag{4.12}$$

$$u_a(p) = \sum_{j=1}^{M_D} \tilde{G}(p, p_j)\mu_j^a \quad \text{and} \quad q_a(p) = \sum_{j=1}^{M_D} \tilde{Q}(p, p_j)\mu_j^a \,, \tag{4.13}$$

where p is the field point where the potential and its normal derivative are evaluated, p_j are the source points, and μ_j^b and μ_j^a are the source densities on the background and the anomaly boundaries, respectively. The diagonal elements for the Neumann boundary condition, in the IBDS formulation, can be determined from the characteristics of the potential function, *i.e.* equation (4.9), and can be expressed as:

$$\tilde{Q}(p_j, p_j) \cong -\frac{1}{l_j} \sum_{i=1, i\neq j}^{M} \tilde{Q}(p_i, p_j) l_i \qquad \text{for } p_j \in \partial(\Omega - \bar{D}). \tag{4.14}$$

It should be noted that for the determination of $\tilde{Q}(p_j, p_j)$ corresponding to the boundary of the anomaly the same procedure should be applied since the problem domain under consideration is a piece-wise homogeneous:

$$\tilde{Q}(p_j, p_j) \cong -\frac{1}{l_j} \sum_{i=1, i\neq j}^{M_D} \tilde{Q}(p_i, p_j) l_i \qquad \text{for } p_j \in \partial D. \tag{4.15}$$

Thus, the EIT boundary conditions in the sense of the CEM, equations (2.31-2.33) and interfacial conditions, equations (2.34), can be expressed as

$$q_b(p_i) = \sum_{j=1}^{M} \tilde{Q}(p_i, p_j) \mu_j^b = 0 \text{ for } p_i \in \partial\Omega_G, \tag{4.16}$$

$$\int_{e_l} \sigma_b q_b(p) dS = I_l \text{ for } l = 1, 2, \cdots, L, \tag{4.17}$$

$$u_b(p_i) + z_l \sigma_b q_b(p_i) = U_l \text{ for } p_i \in e_l \text{ and } l = 1, 2, \cdots, L, \tag{4.18}$$

$$u_b(p_i) = u_a(p_i) \text{ and } q_b(p_i) = -\kappa q_a(p_i) \text{ for } p_i \in \partial\Omega_D, \tag{4.19}$$

where $\kappa = \sigma_a / \sigma_b$.

Integrating equation (4.18) over an electrode and combining equations (4.12), (4.13), and (4.17) we can have

$$\left[\tilde{G}_{EE}\mu_E^b + \tilde{G}_{EG}\mu_G^b + \tilde{G}_{ED}\mu_D^b\right] + \sigma_b \tilde{D}(z_l)\left[\tilde{Q}_{EE}\mu_E^b + \tilde{Q}_{EG}\mu_G^b + \tilde{Q}_{ED}\mu_D^b\right] = C_U U, \tag{4.20}$$

where

$$\tilde{G}_{IJ} = \tilde{G}(p_i, p_j) \ \text{ for } \ p_i \in \partial\Omega_I,\ p_j \in \partial\Omega_J \ \text{ and } \ I, J \in \{E, G, D\}, \tag{4.21}$$

$$\tilde{D}(z_l) = \text{diag}[z_l(p_1), z_l(p_2), \ldots z_l(p_{M_E})] \otimes I_{m_E} \in \Re^{M_E \times M_E} \ , \tag{4.22}$$

$$C_U = \text{eye}(L) \otimes \text{ones}(M_E, 1). \tag{4.23}$$

From the insulation condition, we have

$$\tilde{Q}_{GE}\mu_E^b + \tilde{Q}_{GG}\mu_G^b + \tilde{Q}_{GD}\mu_D^b = 0. \tag{4.24}$$

From the interfacial conditions, we have

$$\tilde{G}_{DE}\mu_E^b + \tilde{G}_{DG}\mu_G^b + \tilde{G}_{DD}\mu_D^b = \tilde{G}_{DD}\mu^a. \tag{4.25}$$

$$\tilde{Q}_{DE}\mu_E^b + \tilde{Q}_{DG}\mu_G^b + \tilde{Q}_{DD}\mu_D^b = -\kappa\tilde{Q}_{DD}\mu^a. \tag{4.26}$$

Integrating the CEM over a certain electrode and imposing the applied current, we have

$$\frac{1}{|e_l|}\int_{e_l} u_b(p)dS + \frac{z_l}{|e_l|} I_l = U_l \ \text{ for } \ l = 1, 2, \cdots, L, \tag{4.27}$$

$$\bar{G}_{LE}\mu_E^b + \bar{G}_{LG}\mu_G^b + \bar{G}_{LD}\mu_D^b + D(z_l / |e_l|)\tilde{I} = U = N\beta, \tag{4.28}$$

$$\begin{aligned} U = N\beta &= N(N^T N)^{-1} N^T \left[\bar{G}_{LE}\mu_E^b + \bar{G}_{LG}\mu_G^b + \bar{G}_{LD}\mu_D^b + D(z_l / |e_l|)\tilde{I} \right] \\ &= \tilde{N}\left[\bar{G}_{LE}\mu_E^b + \bar{G}_{LG}\mu_G^b + \bar{G}_{LD}\mu_D^b + D(z_l / |e_l|)\tilde{I} \right] \end{aligned}, \tag{4.29}$$

where $N_U = \left[\text{ones}(1, L-1); -\text{eye}(L-1)\right]$ and $\beta \in \Re^{(L-1)\times 1}$.

Thus the BDS formulation of the CEM becomes

$$\begin{aligned}&\left[\tilde{G}_{EE}+\sigma_b\tilde{D}(z_l)\tilde{Q}_{EE}\right]\mu_E^b+\left[\tilde{G}_{EG}+\sigma_b\tilde{D}(z_l)\tilde{Q}_{EG}\right]\mu_G^b+\left[\tilde{G}_{ED}+\sigma_b\tilde{D}(z_l)\tilde{Q}_{ED}\right]\mu_D^b\\&=C_U\tilde{N}\left[\bar{G}_{LE}\mu_E^b+\bar{G}_{LG}\mu_G^b+\bar{G}_{LD}\mu_D^b+D(z_l/|e_l|)\tilde{I}\right]\end{aligned},\tag{4.30}$$

$$\begin{aligned}&\left[\tilde{G}_{EE}+\sigma_b\tilde{D}(z_l)\tilde{Q}_{EE}-C_U\tilde{N}\bar{G}_{LE}\right]\mu_E^b+\left[\tilde{G}_{EG}+\sigma_b\tilde{D}(z_l)\tilde{Q}_{EG}-C_U\tilde{N}\bar{G}_{LG}\right]\mu_G^b\\&+\left[\tilde{G}_{ED}+\sigma_b\tilde{D}(z_l)\tilde{Q}_{ED}-C_U\tilde{N}\bar{G}_{LD}\right]\mu_D^b=C_U\tilde{N}D(z_l/|e_l|)\tilde{I}\end{aligned},\tag{4.31}$$

we can express equation (4.31) as

$$V_{EE}\mu_E^b+V_{EG}\mu_G^b+V_{ED}\mu_D^b=C_U\tilde{N}D(z_l/|e_l|)\tilde{I}\,,\tag{4.32}$$

where

$$V_{EE}=\tilde{G}_{EE}+\sigma_b\tilde{D}(z_l)\tilde{Q}_{EE}-C_U\tilde{N}\bar{G}_{LE}\,,\tag{4.33}$$

$$V_{EG}=\tilde{G}_{EG}+\sigma_b\tilde{D}(z_l)\tilde{Q}_{EG}-C_U\tilde{N}\bar{G}_{LG}\,,\tag{4.34}$$

$$V_{ED}=\tilde{G}_{ED}+\sigma_b\tilde{D}(z_l)\tilde{Q}_{ED}-C_U\tilde{N}\bar{G}_{LD}\,,\tag{4.35}$$

$$\bar{G}_{LJ}(l,j)=\frac{1}{|e_l|}\int_{e_l}\tilde{G}(p,p_j)dS\qquad\text{for } J\in\{E,G,D\},\tag{4.36}$$

or

$$\bar{G}_{LJ}=\frac{s_E}{|e|}\left[I_L\otimes ones(1,m_E)\right]\tilde{G}_{EJ}=A\tilde{G}_{EJ}\quad\text{for } J\in\{E,G,D\}.\tag{4.37}$$

Finally, the system of linear equations can be constructed as

$$\begin{bmatrix} V_{EE} & V_{EG} & V_{ED} & 0 \\ \tilde{Q}_{GE} & \tilde{Q}_{GG} & \tilde{Q}_{GD} & 0 \\ \tilde{G}_{DE} & \tilde{G}_{DG} & \tilde{G}_{DD} & -\tilde{G}_{DD} \\ \tilde{Q}_{DE} & \tilde{Q}_{DG} & \tilde{Q}_{DD} & \kappa\tilde{Q}_{DD} \end{bmatrix} \begin{bmatrix} \mu_E^b \\ \mu_G^b \\ \mu_D^b \\ \mu_D^a \end{bmatrix} = \begin{bmatrix} C_U \tilde{N} D(z_l / |e_l|)\tilde{I} \\ 0 \\ 0 \\ 0 \end{bmatrix}. \tag{4.38}$$

4. 2 Hybrid MM of IBDS and SBM

In this section we present the formulation of Hybrid MM which combines IBDS and SBM.

From the formulation of IBDS, equations (4.12) and (4.13) the potential distribution and its normal derivative on the background $\Omega \setminus \bar{D}$ and on the inclusion D can be expressed as

$$u_b(p_i) = \sum_{j=1}^{M} \tilde{G}(p_i, p_j)\mu_j^b = \sum_{j=1, j\neq i}^{M} \tilde{G}_{ij}\mu_j^b + \tilde{G}_{ii}\mu_i^b \ , \tag{4.39}$$

$$q_b(p_i) = \sum_{j=1}^{M} \tilde{Q}(p_i, p_j)\mu_j^b = \sum_{j=1, j\neq i}^{M} \tilde{Q}_{ij}\mu_j^b + \tilde{Q}_{ii}\mu_i^b , \tag{4.40}$$

$$u_a(p_i) = \sum_{j=1}^{M_D} \tilde{G}(p_i, p_j)\mu_j^a = \sum_{j=1, j\neq i}^{M_D} \tilde{G}_{ij}\mu_j^a + \tilde{G}_{ii}\mu_i^a , \tag{4.41}$$

$$q_a(p_i) = \sum_{j=1}^{M_D} \tilde{Q}(p_i, p_j)\mu_j^a = \sum_{j=1, j\neq i}^{M_D} \tilde{Q}_{ij}\mu_j^a + \tilde{Q}_{ii}\mu_i^a , \tag{4.42}$$

where

$$\tilde{G}_{ij} = \tilde{G}(p_i, p_j) = \frac{R_j^2}{2} \ln |p_j - p_i| \quad \text{for} \quad |p_j - p_i| \geq R_j , \tag{4.43}$$

$$\tilde{Q}_{ij} = \tilde{Q}(p, p_j) = -\frac{R_j^2 (p_j - p)\cdot \nu(p)}{2|p_j - p|^2} \quad \text{for} \quad |p_j - p| \geq R_j , \tag{4.44}$$

$$\tilde{Q}_{ii} = \tilde{Q}(p_i, p_i) = -\frac{1}{l_i} \sum_{j=1, j\neq i}^{M} \tilde{Q}(p_j, p_i) l_j \quad \text{for } p_i \in \partial(\Omega - \bar{D}), \tag{4.45}$$

and

$$\tilde{Q}_{ii} = \tilde{Q}(p_i, p_i) = -\frac{1}{l_i} \sum_{j=1, j\neq i}^{M_D} \tilde{Q}(p_j, p_i) l_j \quad \text{for } p_i \in \partial D, \tag{4.46}$$

here, the diagonal terms of $\tilde{G}(p\ , p_j)$ will be determined in a new indirect way, namely an improved inverse interpolation technique used in SBM by Chen *et al.*(2012).

First, let us assume a pure Neumann problem with all the boundary values set as

$$\bar{q}(p) = \frac{\partial \bar{u}(p)}{\partial \nu(p)}\ , \tag{4.47}$$

where $\bar{u}(p)$ (named as sample solution in this paper) is an arbitrary known particular solution, such as

$$\bar{u}(p) = c_1 x + c_2 y\ . \tag{4.48}$$

Then, from the regularized Neumann boundary equation (4.40) or (4.42), we obtain:

$$\bar{q}\ (p_i) = \sum_{j=1, j\neq i}^{M} \tilde{Q}_{ij} \bar{\mu}_j + \tilde{Q}_{ii} \bar{\mu}_i\ , \tag{4.49}$$

where $\bar{\mu}_j$ are unknown coefficients and can be calculated directly by solving the above equation (4.49).

Finally, substituting the calculated $\bar{\mu}_j$ into the Dirichlet boundary equation (4.39) or (4.41), we can get the following algebraic equations:

$$\bar{u}\,(p_i) = \sum_{j=1,\, j\neq i}^{M} \tilde{G}_{ij}\bar{\mu}_j + \tilde{G}_{ii}\bar{\mu}_i + c_0, \tag{4.50}$$

where c_0 is a constant and can be solved by using an arbitrary field point inside the domain. For example, suppose $p_0 = (x_0, y_0)$ is an arbitrary point inside the domain of interest, then the constant c_0 can be calculated by

$$\begin{aligned} c_0 &= \bar{u}(p_0) - \sum_{j=1}^{M} \tilde{G}(p_0, p_j)\bar{\mu}_j \\ &= (c_1 x_0 + c_2 y_0) - \sum_{j=1}^{M} \tilde{G}(p_0, p_j)\bar{\mu}_j \end{aligned} . \tag{4.51}$$

Since the interior field point $p_0 = (x_0, y_0)$ is chosen inside the domain and will never coincide with the boundary source point p_j, the function $\tilde{G}(p_0, p_j)$ can be calculated directly

Thus, diagonal terms of $\tilde{G}(p\ , p_j)$ for Dirichlet boundary equation can be calculated as:

$$\tilde{G}_{ii} = \frac{1}{\bar{\mu}_i}\left[\bar{u}(p_i) - c_0 - \sum_{j=1,\, j\neq i}^{M} \tilde{G}_{ij}\bar{\mu}_j\right], \tag{4.52}$$

i.e.,

$$\tilde{G}_{ii} = \frac{1}{\bar{\mu}_i^b}\left[\bar{u}_b(p_i) - c_0^b - \sum_{j=1,\, j\neq i}^{M} \tilde{G}_{ij}\bar{\mu}_j^b\right] \quad \text{for } p_i \in \partial(\Omega - \bar{D}) \ , \tag{4.53}$$

$$\tilde{G}_{ii} = \frac{1}{\bar{\mu}_i^a}\left[\bar{u}_a(p_i) - c_0^a - \sum_{j=1,\, j\neq i}^{M} \tilde{G}_{ij}\bar{\mu}_j^a\right] \quad \text{for } p_i \in \partial D \, . \tag{4.54}$$

Comparing the formulation of IBDS and Hybrid MM of IBDS and SBM, the only difference is the determination of diagonal terms of $\tilde{G}(p, p_j)$ for Dirichlet boundary equations. Thus, in the calculation of Hybrid MM of IBDS and SBM for EIT forward problems, we just need to replace the expressions of diagonal terms of $\tilde{G}(p, p_j)$ in the formulation. Once the matrix of $\tilde{G}$ and $\tilde{Q}$ are determined then the forward solution can be solved using the equation (4.38).

5. Numerical results and discussion

In this chapter, to verify the feasibility of the IBDS method and the hybrid MM of IBDS and SBM, the numerical results are compared with FEM and BEM. Some numerical examples in 2D circular domain with 16 electrodes attached on the circumference are considered. The background conductivity is set to 3mS/cm. The injected current through electrode 1 is 1 mA and the opposite electrode (electrode 9) is set to a sink, while others are insulated. This corresponds to so-called the opposite current pattern, which is one of widely used current injection protocols. The contact impedance is set to 8 $\Omega \cdot \mathrm{cm}^2$ for all electrodes. As a performance metric, the results are compared to the BEM with more than 10,000 boundary nodes on the boundary. The relative error is computed with respect to the BEM solution and defined as:

$$RE = \frac{\left\| U - \bar{U}_{BEM} \right\|}{\left\| \bar{U}_{BEM} \right\|}, \tag{5.1}$$

where U is the calculated voltage on the electrode using the different forward solvers mentioned before, $\bar{U}_{BEM}$ reference BEM solution with more than 10,000 boundary nodes.

5.1 Homogenous case

Consider a circular domain with homogeneous conditions *i.e*, the conductivity inside the domain is constant through out. The circular domain with outer boundary discretized with 320 uniformly distributed source points is plotted in figure 5.1. The FEM solution used in the comparison for this example is calculated using COMSOL with MATLAB. Figure 5.2 shows the mesh structure used in FEM. The boundary

voltages obtained by the BEM, IBDS and hybrid MM with 320 nodes compared with the FEM solution are plotted in figure 5.3. Figure 5.4 shows the variation of the relative error as the number of source points increases. The BEM solution used as the reference for this example is calculated with 10016 boundary nodes. As seen in figure 5.4, the error for BEM, IBDS and hybrid MM decrease with the increase in number of nodes on domain boundary. BEM involves computation of integrals of fundamental solution over the line segments therefore BEM is computationally intensive compared to IBDS and hybrid MM.

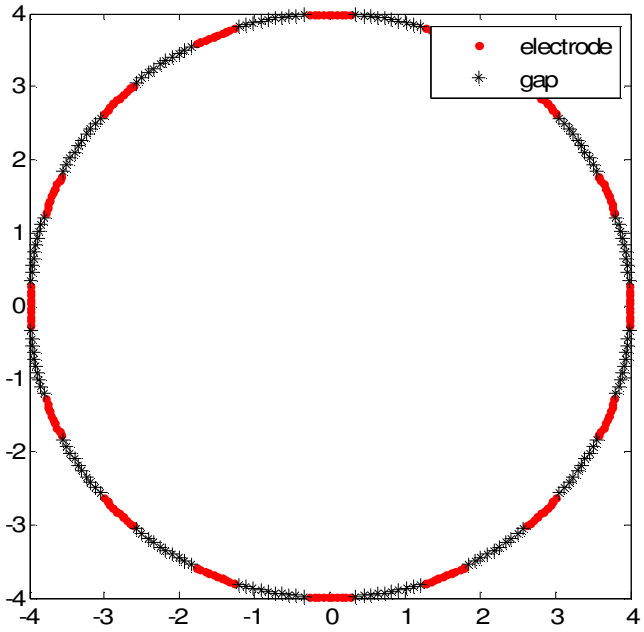

Figure 5.1. Homogenous case with 320 uniformly distributed source points.

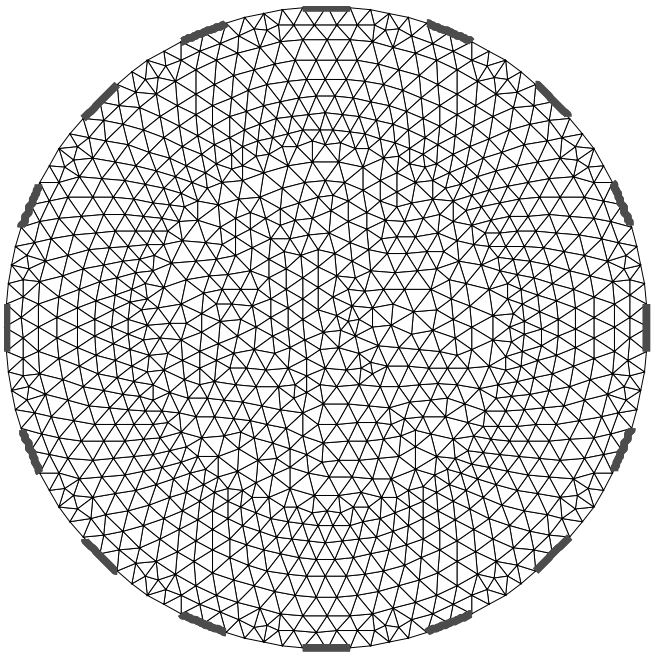

Figure 5.2. Mesh structure used in FEM for homogenous case.

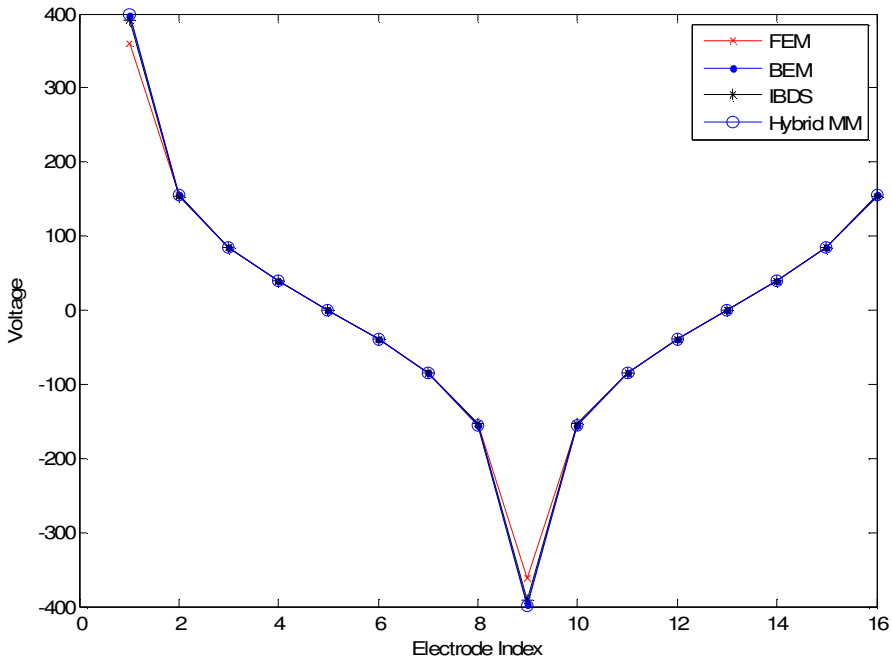

Figure 5.3. Boundary voltages obtained by the BEM, IBDS and hybrid MM with 320 nodes compared with the FEM solution for homogenous case.

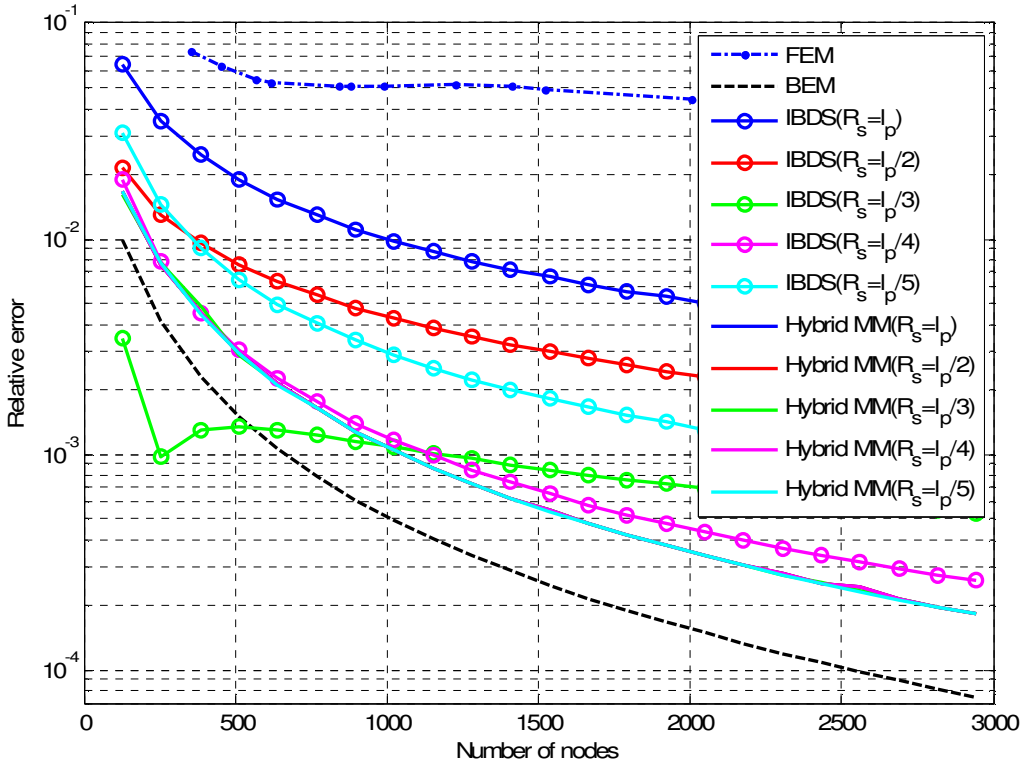

Figure 5.4. Relative error w.r.t the number of elements in FEM and number of boundary nodes in BEM, IBDS and hybrid MM of IBDS and SBM for homogenous case.

As shown in figure 5.3, the voltage calculated from BEM, IBDS and hybrid MM of IBDS and SBM matches well, however the voltage given by FEM has higher deviation compared with the other methods used in the simulation. From figure 5.4, we can find out that the solution given by IBDS is affected by the radius of the source point. In this case, $R_j = l_p / 4$ gives the best result among all the radius of the source point tested in the simulation. Compare to IBDS, the hybrid MM gives better and more stable results. The radius of the source point only shows very small effect on the hybrid MM of IBDS and SBM, it gives almost the same result for different radius of source point.

5.2 Concentric anomaly case

A concentric annular domain is considered as shown in figure 5.5. The concentric case has a circular inclusion with a radius of 2 cm located at the center of the domain. The inclusion is assumed to be a void i.e. $\kappa = 0$. Figure 5.6 shows the mesh structure used in FEM. The boundary voltages obtained by the BEM, IBDS and hybrid MM with 256 points on the outer boundary and 80 points on the inner boundary compared with the FEM solution are plotted in figure 5.7. Figure 5.8 shows the relative error in concentric case with increase in number of nodes in the domain, in which the number of nodes on the boundary of the anomaly is proportional to the number of nodes on the outer boundary, i.e. the ratio of node number on the inner boundary and on the outer boundary is fixed. The BEM solution used as the reference for this example is calculated with 10080 boundary nodes.

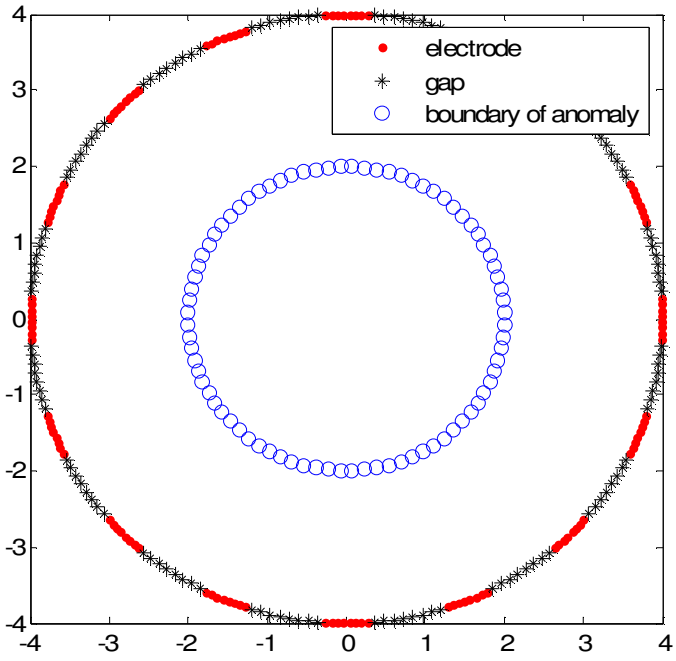

Figure 5.5. Concentric case with 256 source points on the outer boundary and 80 points on the inner boundary.

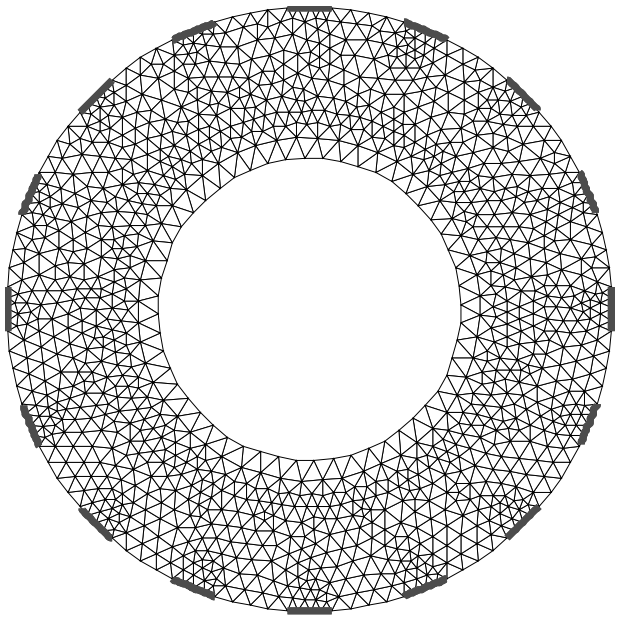

Figure 5.6. Mesh structure used in FEM for concentric anomaly case.

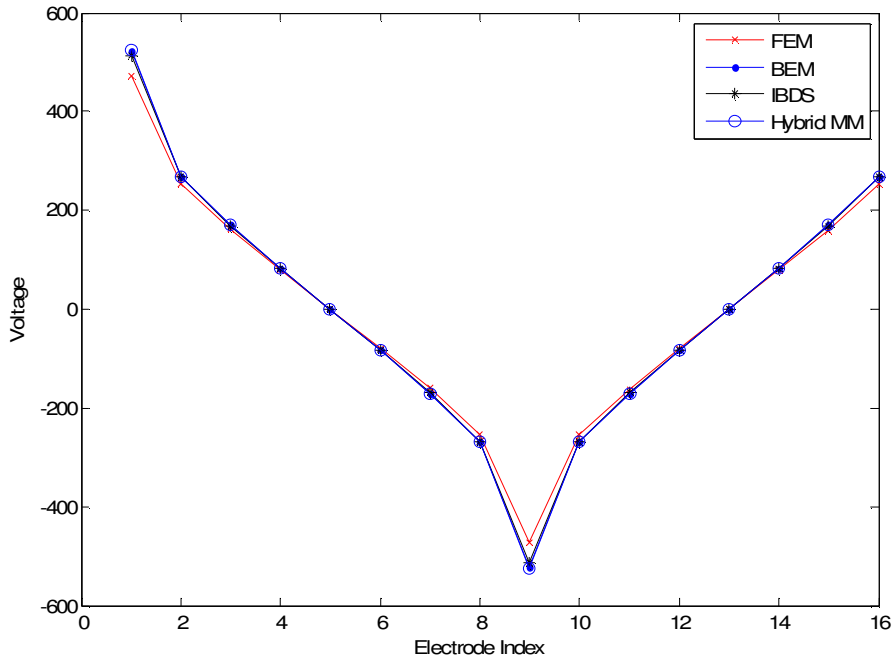

Figure 5.7. Boundary voltages obtained by the BEM, IBDS and hybrid MM compared with the FEM solution for concentric anomaly case.

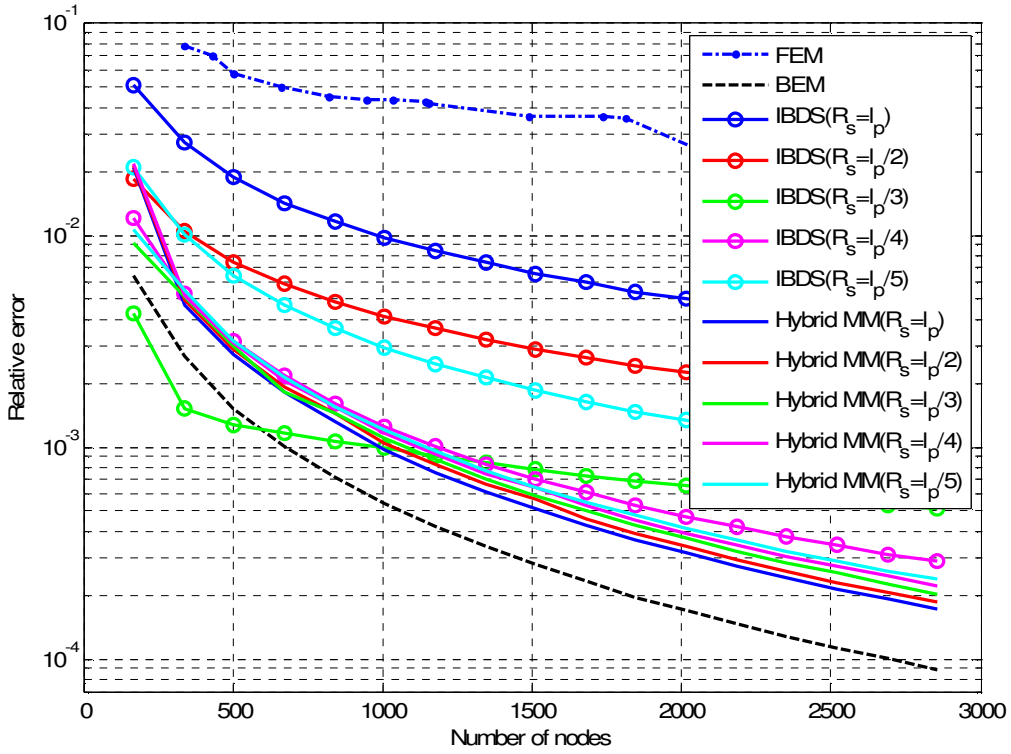

Figure 5.8. Relative error w.r.t the number of elements in FEM and number of boundary nodes in BEM, IBDS and hybrid MM of IBDS and SBM for concentric anomaly case.

For concentric case, it shows the similar feature with the homogenous case. In IBDS, $R_j = l_j / 3$ and $R_j = l_j / 4$ give better results than others, but in the hybrid MM of IBDS and SBM, $R_j = l_j$ gives more accurate result. However, differs form homogenous case the result of hybrid MM of IBDS and SBM is also dependent on the radius of source point like IBDS, this may because of the source points on the outer boundary and inner boundary are not distributed uniformly.

5.3 Circular domain with a Cassini's oval anomaly

As a third example, we select a Cassini's oval as the inclusion (figure. 5.9). The oval is described as

$$r^4 + a^4 - 2a^2 r^2 \cos 2\theta = b^4. \tag{5.2}$$

For $\{a,b\} = \{2, 2.1\}$, the inclusion is assumed to be a void i.e. $\kappa = 0$. Figure 5.10 shows the mesh structure used in FEM. The boundary voltages obtained by the BEM, IBDS and hybrid MM with 256 points on the outer boundary and 100 points on the inner boundary compared with the FEM solution are plotted in figure 5.11. Figure. 5.12 illustrate the relative error with increase in number of nodes in the domain, with fixed ratio of node number on the inner boundary and on the outer boundary. The BEM solution used as the reference for this example is calculated with 10011 boundary points.

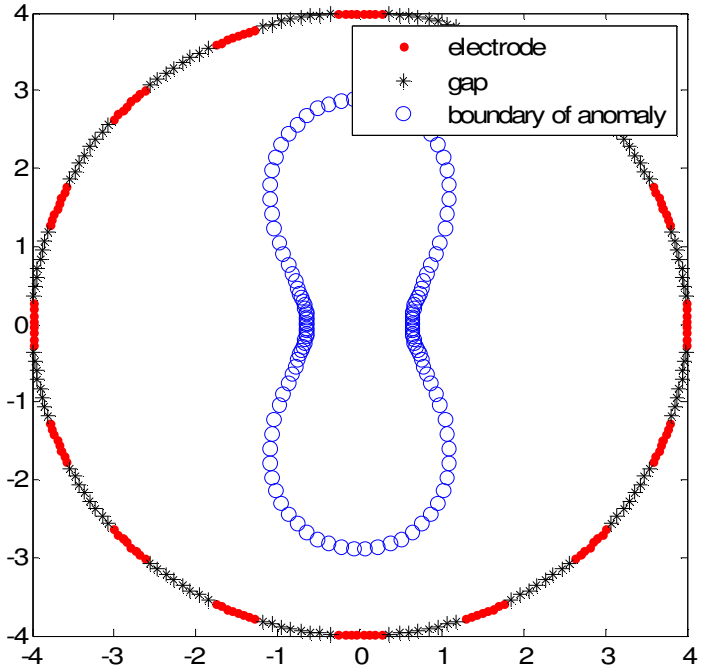

Figure 5.9. Cassini's oval anomaly case with 256 source points on the outer boundary and 100 points on the inner boundary.

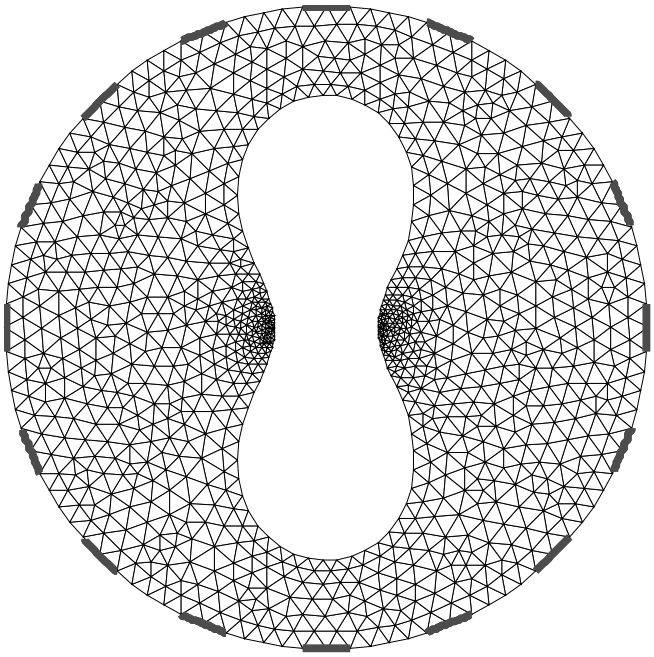

Figure 5.10. Mesh structure used in FEM for Cassini's oval anomaly case.

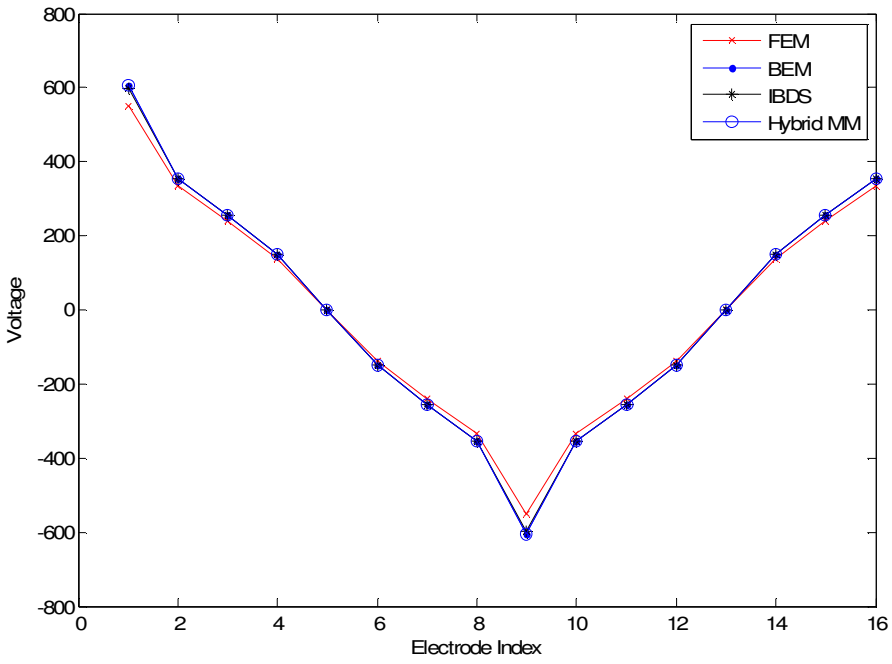

Figure 5.11. Boundary voltages obtained by the BEM, IBDS and hybrid MM compared with the FEM solution for Cassini's oval anomaly case.

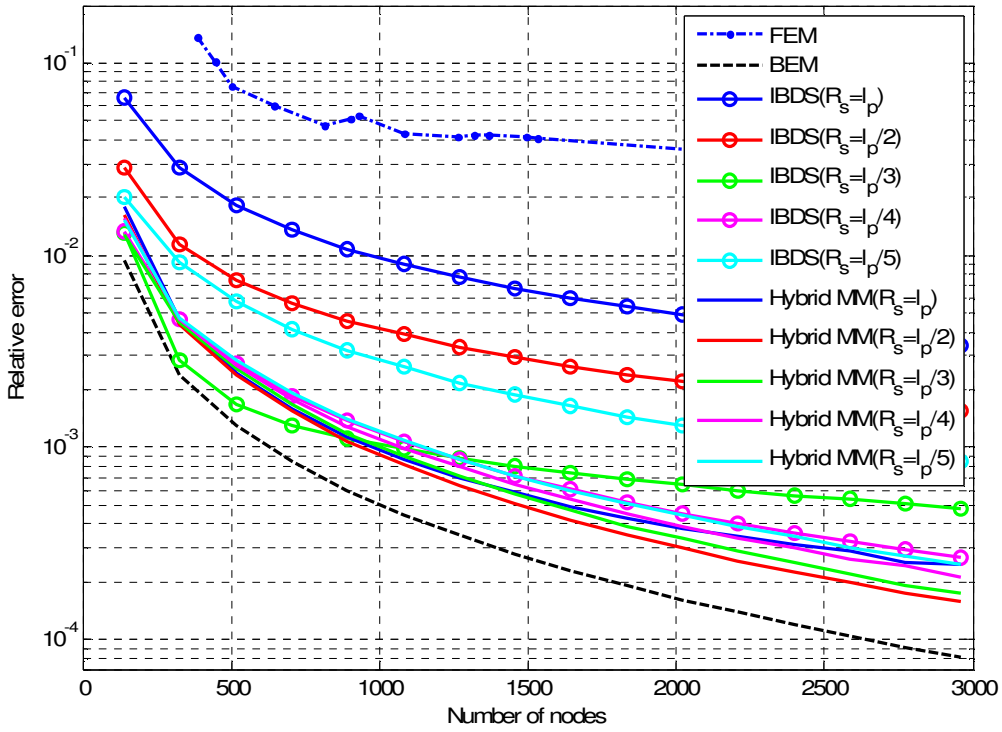

Figure 5.12. Relative error w.r.t the number of elements in FEM and number of boundary nodes in BEM, IBDS and hybrid MM of IBDS and SBM for Cassini's oval anomaly case.

As can be seen in figure 5.9, in this example, the source points are not distributed uniformly and the radius of the distributed source area is not constant but dependent on the location of the source point. From the numerical results, the numerical solution of IBDS is not sensitive to the size of the distributed source area and dependent on the length of the line segment containing the source point.

5.4 Multi-anomaly case

In this section, a circular domain with 3 anomalies is considered. The domain and anomalies with distributed source nodes is plotted in figure. 5.13. As shown in the figure, there are 3 anomalies: an ellipse located at (1, 0) with major and minor axes is

(1, 2); a circle located at (-2, -2) with radius of 1; and a triangle with three vertices located at (-3, 0), (-1, 0) and (-2, 2), respectively. The inclusions are assumed to be a void i.e. $\kappa = 0$. The mesh structure used in FEM is shown in figure 5.14. The boundary voltages obtained by the BEM, IBDS and hybrid MM with 192 source points on the outer boundary and 204 source points on the inner boundary compared with the FEM is shown in figure 5.15. Figure. 5.16 show the relative error with increase in number of nodes in the domain, with fixed ratio of node number on the inner boundary and on the outer boundary.

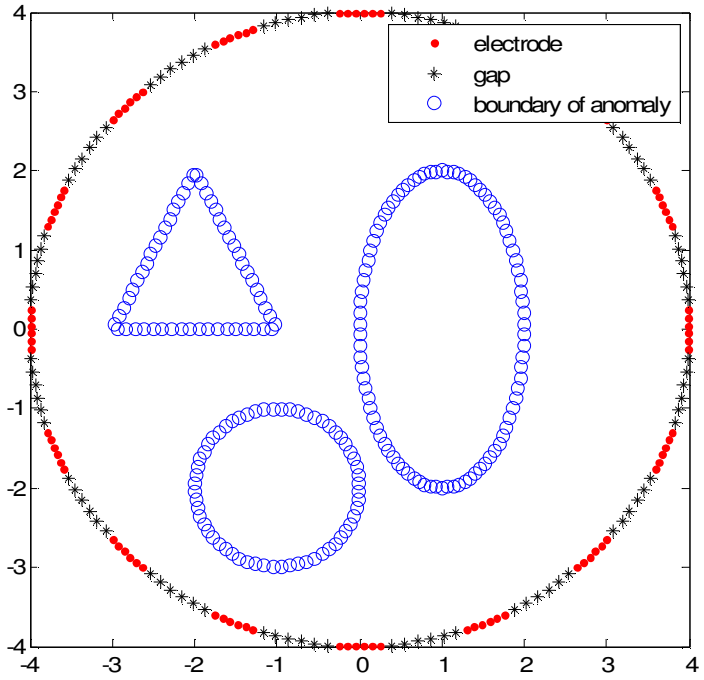

Figure 5.13. Multi-anomaly case with 192 source points on the outer boundary and 204 points on the inner boundary.

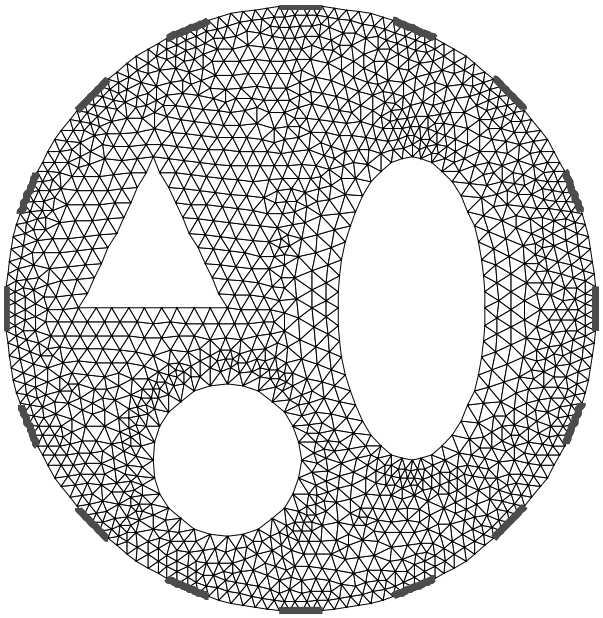

Figure 5.14. Mesh structure used in FEM for multi-anomaly case

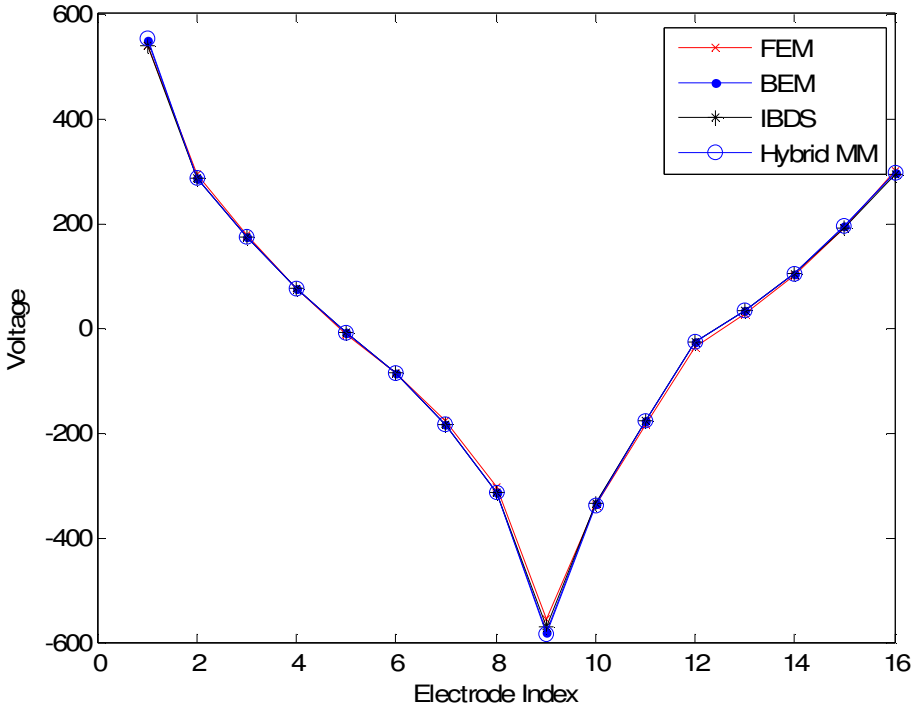

Figure 5.15. Boundary voltages obtained by the BEM, IBDS and hybrid MM compared with the FEM solution for multi-anomaly case.

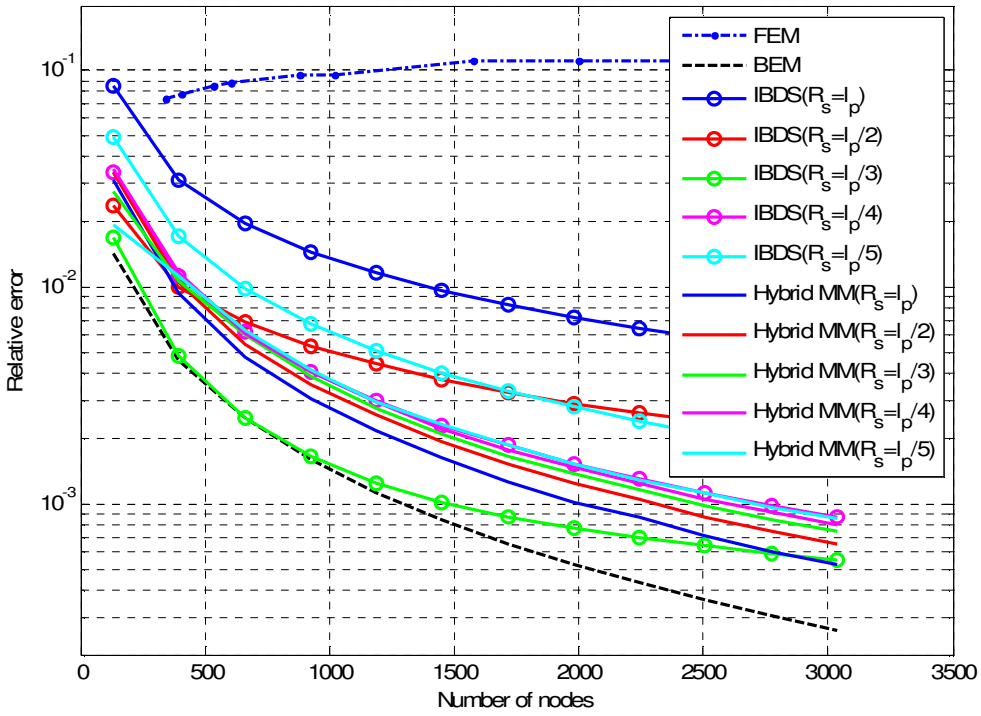

Figure 5.16. Relative error w.r.t the number of elements in FEM and number of boundary points in BEM, IBDS and hybrid MM of IBDS and SBM for multi-anomaly case.

From the numerical experiments reported above, the IBDS is found to be very effective for any complex geometry problem. One limitation of the IBDS is that, similar to the BEM, the system matrix is not sparse therefore this can lead to long computational time when large number of source points is used in the numerical simulation. Compare to IBDS, the hybrid MM of IBDS and SBM show higher accuracy and it is less dependent on the radius of the source points, in other words, we can say that the hybrid MM of IBDS and SBM is more effective and more stable. But, the drawback of the hybrid MM of IBDS and SBM is the choice of the particular solution, some times the result is sensitive to the particular solution we used in the calculations of the diagonal terms for Dirichlet boundary equations.

6. Conclusions

This study considers an improved formulation of the BDS method in order to obtain the numerical solution for the forward problem of the EIT with the complete electrode model, which corresponds to a combination of Laplace equations on a piece-wise homogeneous media subject to the mixed boundary conditions with integral constraints. By combining the inverse interpolation technique used in SBM, a hybrid MM of IBDS and SBM is proposed and the formulation for forward problem of EIT is derived.

Several numerical examples are tested to demonstrate the feasibility and accuracy of the new formulation by comparing the simulation results with BEM and the FEM with linear basis functions. The results show that the accuracy of the hybrid MM is better than IBDS. Furthermore, the IBDS and the hybrid MM of IBDS and SBM are found to be very effective for any complex geometry problem. One limitation of the IBDS is that, similar to the BEM, the system matrix is not sparse therefore this can lead to long computational time when large number of source points is used in the numerical simulation. Compare to IBDS, the hybrid MM of IBDS and SBM show higher accuracy and it is less dependent on the radius of the source points, in other words, we can say that the hybrid MM of IBDS and SBM is more effective and more stable.

But, the drawback of the hybrid MM of IBDS and SBM is, similar to SBM, the choice of the particular solution. Some times the result is sensitive to the particular solution we used in the calculations of the diagonal terms for Dirichlet boundary equations.

The present work is focused on two-dimensional forward problem and it's extending to 3D is straight forward. The currently employed numerical method for forward problem of EIT is applicable to other kind of PDEs with complex geometry.

Future work can include finding appropriate source radius, improvement of the IBDS solution as still the BEM solution is found to have less error compared to IBDS solution, and the extension of the IBDS and the hybrid MM to forward problem in three dimension and inverse problem in EIT such as boundary estimation problems.

Summary

Meshless methods or mesh-free methods (MMs) are a kind of numerical methods developed with the objective of avoiding part of the disadvantages associated with reliance on a mesh to construct the approximate solution. In MMs, the approximation is built from nodes only, thus, the MMs are particularly suitable for problems with complex geometries, like domains involving internal boundaries for instance. Among the MMs, the method of fundamental solutions (MFS) has gained an increasing attention in many engineering and science fields. In MFS, the solution of the problem is approximated as a linear combination of fundamental solutions of the governing equation. However, the conventional MFS requires a fictitious boundary outside the physical domain to place the source points due to singularities of the fundamental solution, and the determination of fictitious boundary is momentous in solving the problem. To overcome this main demerit of the conventional MFS, several methods such as the modified method of fundamental solution (MMFS), singular boundary method (SBM) and the boundary distributed source (BDS) method have been proposed. The MMFS, SBM and BDS overcome the artificial boundary in the conventional MFS by distributing the source point on the physical boundary as well as the field points. The key point of SBM is to evaluate the origin intensity factor to isolate the singularity of the fundamental solution based on subtracting and adding-back technique as well as the inverse interpolation technique (IIT). The main idea of the BDS method is to avoid the singularities of the fundamental solution at source points by considering integration over a distributed source within circles in two-dimensional (2D) or spheres in three-dimensional (3D). The improved BDS method, namely IBDS method uses a simpler way to determine the diagonal elements for the Neumann boundary conditions by invoking the fact that the boundary integration of the normal gradient of the potential should vanish.

Electrical Impedance Tomography (EIT) is an imaging technique which reconstructs the shape and the location of inclusions with different electrical conductivity based on the voltage measurements excited by the currents injected

through the electrodes attached on the domain boundary. The EIT forward problem is a sort of the Laplace equation on the piece-wise homogeneous domain subject to the mixed boundary conditions with constraints of integral form, it can be applicable in industrial and medical tomography applications where the interest is to determine the distribution of conductivity in the domain or the shape reconstruction.

This study presents a novel meshless method (MM) which combines SBM and IBDS to obtain the numerical solution for the EIT forward problem. The IIT used in SBM is employed to determine the diagonal elements for the Dirichlet boundary conditions. By employing the IBDS method and the novel MM which combines SBM and IBDS, the mathematical formulation of EIT forward problem for complete electrode model (CEM) is derived. Several numerical examples are tested to demonstrate the feasibility and accuracy of the new formulation by comparing the simulation results with BEM and FEM.

The results show that the accuracy of the hybrid MM is better than IBDS. Furthermore, the IBDS and the hybrid MM of IBDS and SBM are found to be very effective for any complex geometry problem. Compare to IBDS, the hybrid MM of IBDS and SBM show higher accuracy and it is less dependent on the radius of the source points, in other words, we can say that the hybrid MM of IBDS and SBM is more effective and more stable. Therefore, it is expected that this method can be used to solve wide variety of applications in EIT.

References

Abascal J, Arridge S, Lionheart W, Bayford R and Holder D, 2007 Validation of a finite-element solution for electrical impedance tomography in an anisotropic medium, *Physiol. Meas.,* 28 S129-S140

Andrew P.B. et al., 2003 Electrical resistance tomography of human brain function using reconstruction algorithms based on the finite element method, *NeuroImage*, 20 752-764.

Atluri S N, Shen S P, 2005 The basis of meshless domain discretization: the meshless local Petrov–Galerkin (MLPG), *method. Adv. Comput. Math.*, 23 73-93

Atluri S N, Shen S, 2002 *The Meshless Local Petrov-Galerkin (MLPG) Method*, Tech Science Press, Stuttgart

Atluri S N and Zhu T, 1998 A new meshless local Petrov-Galerkin (MLPG) approach in computational mechanics, *Comput. Mech.,* 22 117-27

Alves C J S, Leitão V M A, 2006 Crack analysis using an enriched MFS domain decomposition technique, *Eng. Analysis Bound. Elements*, 30 160-166

Barker R D and Moore J, 1998 The application of time-lapse electrical tomography in groundwater studies, *The Leading Edge* 17 1454-1458

Belytschko T, Krongauz Y, Organ D, Fleming M, Krysl P, 1996 Meshless Methods: An Overview and Recent Developments, *Comp. Methods Appl. Mech. Engrg.*, 139 3-47

Belytschko T, Guo Y, Liu W K, Xiao S P, 2000 A unified stability analysis of meshfree particle methods, *Int. J. Numer. Methods Eng.*, 48 1359-1400.

Bodin A, Ma J, Xin X J, Krishnaswami P, 2006 A meshless integral method based on regularized boundary integral equation, *Comput. Methods Appl. Mech. Engrg.*, 195 6258-6286

Bogomolny A, 1985 Fundamental solutions method for elliptic boundary value problems, *SIAM Journal on Numerical Analysis*, 22 644-669

Bonet J, Kulasegaram S, 2000 Correction and stabilization of smooth particle hydrodynamics methods with application in metal forming simulations, *Int. J. Numer. Methods Eng.,* 47 1189-1214.

Borcea L, 2002 Electrical impedance tomography, *Inverse Prob.* 18 R99-R136

Brown B H, Barber D C, Morica A H and Leathard A D, 1994 Cardiac and respiratory related electric impedance changes in the human thorax, *IEEE Trans. Biomed. Eng.,* 41 729-723.

Brown B H, 2001 Medical impedance tomography and process impedance tomography: a brief review, *Meas. Sci.Technol.,* 12 991-6

Casas A, Himi M, Diaz Y, Pinto V, Font X and Tapias J C, 2008 Assessing aquifer vulnerability to pollutants by electrical resistivity tomography (EIT) at a nitrate vulnerable zone in NE Spain, *Environ. Geol.,* 54 515-520

Cartwright D J, 2001 Underlying Principles of the Boundary Element Method, Billerica, MA: *Computational Mechanics*

Chati M K, Mukherjee S, Mukherjee Y X, 1999 The boundary node method for three-dimensional linear elasticity, *Int. J. Numer. Methods Engrg.*, 46 1163-1184

Chen J S, Liu W K, 2000 Meshless particle methods. *Comput. Mech.*, 25 99-317

Chen J T, Chang M H, Chen K H, Lin S R, 2002a The boundary collocation method with meshless concept for acoustic eigenanalysis of two-dimensional cavities using radial basis function, *J. Sound. Vib.,* 257 667-711

Chen J T, Chang M H, Chen K H, Chen I L, 2002b Boundary collocation method for acoustic eigenanalysis of three-dimensional cavities using radial basis function, *Comput. Mech.*, 29 392-408

Chen K, Kao J, Chen J, Young D, Lu M, 2006 Regularized meshless method for multiply-connected-domain Laplace problems, *Engineering Analysis with Boundary Elements*, 30 882-896

Chen W, 2009 Singular boundary method: a novel, simple, meshfree, boundary collocation numerical method, *Chin. J. Solid. Mech.,* 30 592-599

Chen W and Wang F Z, 2010 A method of fundamental solutions without fictitious boundary, Eng. Anal. Bound. Elem., 34 530-532

Chen W, Fu Z J and Wei X, 2009 Potential problems by singular boundary method satisfying moment condition, *Comput. Model. Eng. Sci.,* 54 65-85

Chen W, Tanaka M, 2002 A meshfree, integration-free and boundary-only RBF technique, Comput. Math. Appl. 43 379-391

Chen W, Wang F Z, 2010 A method of fundamental solutions without fictitious boundary, *Engineering Analysis with Boundary Elements* 34 530-532

Chen J S, Liu W K, 2004 Meshless methods: Recent advances and new applications, *Comp. Methods Appl. Mech. Engrg.* 193 933-1321

Chen W, Gu Y, 2012 An improved formulation of singular boundary method, *Advances in Applied Mathematics and Mechanics* 4 543-558

Cheng A, 2000 Particular solutions of Laplacian, Helmholtz-type, and polyharmonic operators involving higher order radial basis functions, *Eng. Anal. Bound. Elem.*, 24 531–538

Cheng K.S., Isaacson D., Newell J.C., Gisser D.G., 1998 Electrode models for electric current computed tomography, *IEEE Trans. Biomed. Eng.*, 36 918-924.

Cherepenin V A, Karpov A, Korjenevsky A, Kornienko V, Mazaletskaya A and Mazourov D, 2001 A 3D electrical impedance tomography (EIT) system for breast cancer detection, *Physiol. Meas.,* 22 9-18

Cherepenin V A, Karpov A Y, Korjenevsky A V, Kornienko V N, Kultiasov Y S, Ochapkin M B, Trochanova O V, and Meister J D, 2002 Three-dimensional EIT imaging of breast tissues: System design and clinical testing, *IEEE Trans. Med. Imag.,* 21 662-667

Chinnaboon B, Katsikadelis J T and Chucheepsakul S, 2007 A BEM-based meshless method for plates on biparametric elastic foundation with internal supports, *Comput. Methods Appl. Mech. Engrg.,* 196 3165-3177

Choi M H, Kao T J, Isaacson D, Saulnier G J and Newell J C, 2004 A simplified model of mammography geometry for breast cancer imaging with electrical impedance tomography, in *Proc. 26th Annu. Int. Conf. IEEE EMBS*, San Francisco 1310-1313

de Munck J, Faes T and Heethaar R, 2000 The Boundary Element Method in the Forward and Inverse Problem of Electrical Impedance Tomography, *IEEE Transactions on Bomedical Egineering*, 47 792-800

Daily W, Ramirez A, 1992 Electrical resistivity tomography of vadose water movement *water resource research,* 28 1429-1442

Deibele J M, Luepschen H and Leonhardt S 2008 Dynamic separation of pulmonary and cardiac changes in electrical impedance tomography *Physiol. Meas.* 29 S1-14.

Dickin F and Wang M, 1996 Electrical resistance tomography for process tomography *Meas.Sci.Technol,* 7 247-260

Duraiswami R, Chahine G and Sarkark, 1997 Boundary Element Techniques for 2-D and 3-D Electrical Impedance Tomography, *Chemical Engineering Science*, 52 2185-2196

Fairweather G, Karageorghis A, 1998 The method of fundamental solutions for elliptic boundary value problems, *Adv. Comput. Math.*, 69-95

Friedman A and Vogelius M, 1989 Determining cracks by boundary measurements *Indiana University Mathematics Journal*,38 527-556

Fries T P and Matthies H G, 2004 *Classification and Overview of Meshfree Methods*, Brunswick, Germany

Gingold R A, Monaghan J J, 1977 Smoothed particle hydrodynamics: theory and application to non-spherical stars, Monthly Notices, *R. Astron. Soc,.* 181 375-389

Griebel M, Schweitzer M A, 2002 *Meshfree Methods for Partial Differential Equations*, Springer Verlag, Berlin

Gu Y, Liu G, 2005 Meshless Methods Coupled with Other Numerical Methods, *Tsinghua Science and Technology*, 10 8-15

Gu Y, Chen W and Zhang C Z, 2011 Singular boundary method for solving plane strain elastostatic problems, *Int. J. Solids Struct.*, 48 2549-2556

Gu Y T, Liu G R, 2002 A boundary point interpolation method for stress analysis of solids, Comput. Mech. 28 47-54

Gu Y, Chen W, Zhang J, 2012 Investigation on near-boundary solutions by singular boundary method, Engineering Analysis with Boundary Elements, 36 1173-1182

Harris N D 1991 Applications of electrical impedance tomography in respiratory medicine *PhD Thesis* Univ. of Sheffield

Hanke M, Brühl M, 2003 Recent progress in electrical impedance tomography, *Inverse Prob,* 19 S65-S90

Hakula H, Hyvon N, Tuominen T, 2012 On the hp-adaptive solution of complete electrode model forward problems of electrical impedance tomography, *Journal of Computational and Applied Mathematics*, 236 4645-4659

Holder D S, 1992 Electrical impedance tomography (EIT) of brain function *Brain Topogr.,* 5 87-93

Hwang W, Hung L, Ko C, 2002 Non-singular boundary integral formulations for plane interior potential problems, *Int. J. Numer. Meth. Eng.*, 53 1751-1762

Jalaal M, Soheil S, Domairry G, Ghasemi E, Bararnia H, Mohammadi F, Barari A, 2011 Numerical simulation of electric field in complex geometries for different electrode arrangements using meshless local MQ-DQ method, *Journal of Electrostatics*, 69 168-175

Jain H, Isaacson D, Edic P M and Newell J C, 1997 Electrical impedance tomography of complex conductivity distributions with noncircular boundary, *IEEE Trans. Biomed. Eng.,* 44 1051-1060

Jones O C, Lin J T, Ovacik L and Shu H, 1993 Impedance imaging relative to gas-liquid systems, *Nuclear Engineering and Design,* 141 159-176

Kansa E J, 1990 A scattered data approximation scheme with application to computational fluid-dynamics—I &II, *Comput. Math. Appl.*, 19 127-61

Karageorghis A, Lesnic D, Marin L, 2011 A survey of applications of the MFS to inverse problems, *Inv. Prob. Sci. Eng.,* 2011 309-36

Katsurada M, Okamoto U, 1996 The collocation points of the fundamental solution method for the potential problem, *Computers and Mathematics with Applications*, 31 123-137

Khambampati A K, Lee B A, Kim K Y and Kim S, 2012 An analytical boundary element integral approach to track the boundary of a moving cavity using electrical impedance tomography, *Meas. Sci. Technol.* , 23 035401 (17pp)

Khambampati A K, Kim S and Kim K Y, 2011 An EM algorithm for dynamic estimation of interfacial boundary in stratified flow of immiscible liquids using EIT, *Flow Measurement and Instrumentation*, 22 517-528

Khambampati A K, Rashid A, Kim S, Soleimani M and Kim K Y, 2009 Unscented Kalman filter approach to track moving interfacial boundary in sedimentation process using three-dimensional electrical impedance tomography, *Proc. R. Soc. A.,* 367 3095-3120

Kerner T E, Paulsen K D, Hartov A, Soho S K and Poplack S P, 2002a Electrical impedance spectroscopy of the breast: clinical results in 26 subjects, *IEEE Trans. Med. Imag.,* 21 638-45.

Kerner T E, Hartov A, Soho S K, Poplack S P and Paulsen K D, 2002b Imaging the breast with EIS: an initial study of exam consistency, *Physiol. Meas.,* 23 221-36

Kim B S, Boverman G, Newell J C, Saulnier G J and Isaacson D, 2007 The complete electrode model for EIT in mammography geometry, *Physiol. Meas.,* 28 S57-S69

Kim K Y, Kim B S, Kim M C, Kim S, 2004 Dynamic inverse obstacle problems with electrical resistance tomography, *Mathematics and Computers in Simulation*, 66 399-408

Kim S, 2013 An improved boundary distributed source method for two-dimensional Laplace equations, *Engineering Analysis with Boundary Elements,* 37 997-1003

Lee B A, 2012 *Development of a Computational Analysis System for Electrical Impedance Tomography*, Ph.D. Thesis, Jeju National University, Korea

Liu C S, 2012 An equilibrated method of fundamental solutions to choose the best source points for the Laplace equation, *Engineering Analysis with Boundary Elements*, 36 1235-1245

Li S, Liu W K, 2002 Meshfree and particle methods and their applications, *Appl. Mech. Rev.* 55 1-34

Liu G R, 2002 *Meshless Methods*, CRC Press, Boca Raton

Liu W K, Belytschko T, Oden J T, 1996 Meshless methods, *Comp. Methods Appl. Mech. Engrg.,* 139 1-400

Liu Y, 2010 A new boundary meshfree method with distributed sources, *Engineering Analysis with Boundary Elements,* 34 914-919

Lucy L B, 1977 A numerical approach to the testing of the fission hypothesis, *Astron. J.*, 82 1013-1024.

Maillol J M, Seguin M K, Gupta O P, Akhauri H M and Sen N, 1999 Electrical resistivity tomography survey for delineating uncharted mine galleries in West Bengal, India, *Geophys. Prospect., Eur. Assoc. Geosci. Eng.,* 47 103-116

Mann R, Dickin F J, Wang M, Dyakowski T, Williams R A, Edwards R B, Forrest A E and Holden P J, 1997 Application of electrical resistance tomography to interrogate mixing processes at plant scale, *Chem. Eng. Sci,.* 52 2087-2097

Mathon R, Johnston R L, 1977 The approximate solution of elliptic boundary-value problems by fundamental solutions, *SIAM Journal on Numerical Analysis,* 14 638-650

Meads L N, Bently L R, Mendoza C A, 2003 Application of electrical resistivity imaging to the development of a geological model for a proposed Edmonton landfill site, *Canadian Geotechnical Journal.,* 40 499-523

Monaghan J J, 1982 Why particle methods work, *SIAM J. Sci. Stat. Comput.,* 3 422-433.

Melenk J M and Babuska I, 1996 The partition of unity finite element method: Basic theory and applications, *Computer Methods in Applied Mechanics and Engineering.,* 139 289-314

Mueller J L, Isaacson D and Newell J C, 2001 Reconstruction of conductivity changes due to ventilation and perfusion from EIT data collected on a rectangular electrode array, *Physiol. Meas.,* 22 97-106

Mukherjee Y X, Mukherjee S, 1997 Boundary node method for potential problems, *Int. J. Numer. Methods Engrg.,* 40 797-815

Osterman K S, Kerner T E, Williams D B, Hartov A, Poplack S P and Paulsen K D, 2000 Multifrequency electrical impedance imaging: preliminary in vivo experience in breast, *Physiol. Meas.,* 21 99-109

Perne M, Šarler B, Gabrovšek F, 2012 Calculating transport of water from a conduit to the porous matrix by boundary distributed source method, *Engineering Analysis with Boundary Elements,* 36 1649-1659

Pinheiro P A T, Loh W W and Dickin F J, 1997 Smoothness-constrained inversion for two-dimensional electrical resistance tomography, *Meas. Sci.Technol.*, 8 293-302

Polydorides N and Lionheart WRB, 2002 A MATLAB toolkit for three-dimensional electrical impedance tomography: A contribution to the electrical impedance and diffuse optical reconstruction software project, *Meas. Sci. Technol.,* 13 1871-1883

Rashid A, Kim B S, Khambampati A K, Liu Dong, Kim S and Kim K Y 2010 Dynamic boundary estimation of human heart within a complete cardiac cycle using electrical impedance tomography, *J. Phys.: Conf. Ser.,* 224 012042

Rek Z, Šarler B, 1999 Analytical integration of elliptic 2D fundamental solution and its derivatives for straight-line elements with constant interpolation, *Engineering Analysis with Boundary Elements,* 23 515-525

Reynolds J M, Taylor D I, 1996 Use of geophysical surveys during the planning, construction and remediation of landfills in S.P. Bentley *Engineering Geology of waste disposal: The Geological society of London,* 11 93-98

Saavedra I, Power H, 2003 Multi pole fast algorithm for the least-squares approach of the method of fundamental solutions for three-dimensional harmonic problems, *Numer. Methods Partial Differential Equation*, 828-45

Šarler B, 2009 Solution of potential flow problems by the modified fundamental solutions: Formulations with the single layer and the double layer fundamental solutions, *Engineering Analysis with Boundary Elements,* 33 1374-1382

Shigeta T, Young DL, 2009 MFS for the Laplace equation Method of fundamental solutions with optimal regularization techniques for the Cauchy problem of the Laplace equation with singular points, *Journal of Computational Physics*, 228 1903-1915

Smyrlis Y S, Karageorghis A, 2001 Some aspects of the method of fundamental solutions for certain harmonic problems, *J. Sci. Comput.*, 41-71

Somersalo E., Cheney M and Isaacson D, 1992 Existence and uniqueness for electrode models for electric current computed tomography, *SIAM J. Appl. Math.*, 52 23-40

Tsai C C, Young D L, Chiang J H, Lo D C, 2006 The method of fundamental solutions for solving options pricing models, *Applied Mathematics and Computation*, 181 390-401

Swegle L W , Hicks D L, 1995 Attaway S W, Smooth particle hydrodynamics stability analysis, *J. Comput. Phys.*, 116 123-134.

Spies B and Ellis R 1995 Cross-borehole resistivity tomography of a pilot scale, insitu verification test, *Geophysics,* 60 886-898

Sukumar N, Moran B, Belytschko T, 1998 The natural element method, *Int. J. Numer. Methods Engrg.*, 43 829-887

Tournour M, Atalla N, 1999 Efficient evaluation of the acoustic radiation using multipole expansion, *Int. J. Numer. Meth. Eng.*, 46 825-837

Uhlmann G, 2009 Electrical impedance tomography and Calderón's problem, *Inverse Prob.,* 25 123011

Vauhkonen M., *Electric Resistance Tomography and Prior Information*, Ph.D. Thesis, Kupio University, Finland, 1997 13-45.

Wang J G, Xie H, Leung C F, 2009 A local boundary integral-based meshless method for Biot's consolidation problem, *Eng. Ana. with Bound. Elem.,.* 33 35-42

Wang J G, Liu G R, 2002 A point interpolation meshless method based on radial basis functions, *Int. J. Numer. Methods Eng.,* 54 1623-48

Xiao S P, Belytschko T, 2005 Material stability analysis of particle methods, *Adv. Comput. Math.,* 23 171-190

Young D L, Chen K H, Lee C W, 2005 Novel meshless method for solving the potential problems with arbitrary domain, *Journal of Computational Physics,* 209 290-321

Young D L, Chen C W, Fan C M, Murugesan K and Tsai C C, 2005 The method of fundamental solutions for Stokes flow in a rectangular cavity with cylinders, *European Journal of Mechanics B/Fluids*, 24 703-716

Young D L, Chiua C L, Fan C M, Tsai C C, Lin Y C, 2006 Method of fundamental solutions for multidimensional Stokes equations by the dual-potential formulation, *European Journal of Mechanics B/Fluids*, 25 877-893

Young D L, Tsai C C, Chen C W, Fan C M, 2008 The method of fundamental solutions and condition number analysis for inverse problems of Laplace equation, *Computers and Mathematics with Applications*, 55 1189-1200

Zhang Z, Zhao P, Liew K, 2009 Improved element-free Galerkin method for two-dimensional potential problems, *Engineering Analysis with Boundary Elements*, 33 547-554

Zhu T, Zhang J D, Atluri S N, 1998 A local boundary integral equation (LBIE) method in computational mechanics, and a meshless discretization approach, *Comput. Mech.*, 21 223-35